

BEAM KNEES AND OTHER BRACKETED CONNECTIONS

by

Prof. Ir. H. E. JAEGER and Ir. J. J. W. NIBBERING

Publication Nr. 9 of the Ship Structure Laboratory, Technological University, Delft

Summary

This report describes the work carried out in the Ship Structure Laboratory of the Technological University, Delft, Netherlands, by the authors, in order to clarify the behaviour of beam knees and other bracketed connections under dynamic and static loads.

The report first gives a general view of the function of a beam knee or bracket in the structure of a ship. It explains the theory underlying the behaviour and influence of bracketed connections as applied to ship's structural problems and the necessity of investigating dynamic load influence by tests.

The results of static and dynamic tests are analysed and a general view is given on the construction of adequate bracketed joints. Some tests give information about effective beam knee-connections, without the use of bracket- or gusset plates, by butt welding orthogonally connecting adjacent members.

An approximate calculation method is given for predicting bracket stresses.

Parts of this report were published by the authors in the bulletin of the "Association Technique Maritime et Aéronautique", Paris, in 1959 and 1960 [17] and [18].

§ 1. Introduction

When riveting was the normal way of connecting two ship's members, bracketed joints were used to connect structural members orthogonally to each other. In particular, beams and frames, but also stiffeners and beams, longitudinals and stiffeners, were joined by brackets or knees.

Two orthogonally connected beams were supposed to form in this way a stiff connection, so that no change in the angle between the two beams was possible. This, of course, is only true as long as the loads don't bring the construction into the plastic range.

The bracket itself had to be strong enough to take up and transmit the applied forces and moments without risk of collapse or overstressing.

The improvement of welding techniques made the riveted knee a rarity. On the other hand, in welded bracketed connections the desired stiffness of the angle between the respective structural members is no problem. It seems then possible to do away with the bracket plate in the corner altogether and to weld two orthogonally adjacent beams at their joints by butt welds. And as mentioned, this corner represents a very stiff connection.

It is clear that the *first function* of the knee-plate viz. maintaining the axes of the respective members at the same angle one to another, becomes less important. The next step is now to make the corner connection more modern.

Therefore, constructing the bracket-connection as it was in the days of riveting has no sense, and the question arises, how to achieve the *second goal* of the welded knee-connection viz. to lead the stresses smoothly around the corner, created by the two orthogonally butt welded beams. This cannot be done with the old-fashioned brackets and beam-knees. The solution would thus be the creation of

what is called in this report: "The ideal knee" (fig. 4).

Opie [1] gives a short explanation of the influence of brackets on the end-connections of beams and observes that with bracketed connections an important effect is introduced by the presence of the brackets as such on the bending moments in a fully or partially constrained beam at its ends.

But in the welded bracketed connection the smoothing of the stresses becomes of more importance since the welded corner without bracket would even be an acceptable possibility. But the relatively small strength of this corner, when the angle is submitted to an "opening" traction, makes it advisable to use a knee. And this traction is very often present with dynamic loads.

The welded knee therefore must be investigated by dynamic tests in order to find its most advantageous form. Therefore the comparison with an "ideal knee" is indicated (see § 9).

A *third function* of the bracketed knee-connection is the aid these structural members give during the erection on the stocks. In this function the overlapping knee-plate is often used. From the point of view of welded construction this overlap must be condemned very strongly. The knee in this form, as well as asymmetrical profiles, is a relic of the times of riveting and the plea for its necessity as auxiliary for the mounting of sections is also erroneous. It is much better to make the connections of the limiting edges of the sections at places where no corners, discontinuities and complicated welded constructions are present. Figures 1 and 2 give some examples of well-designed section-edges in this respect.

Summarizing we see that knee-brackets have three distinct functions, the respective importance of which changed, when the bracketed connection

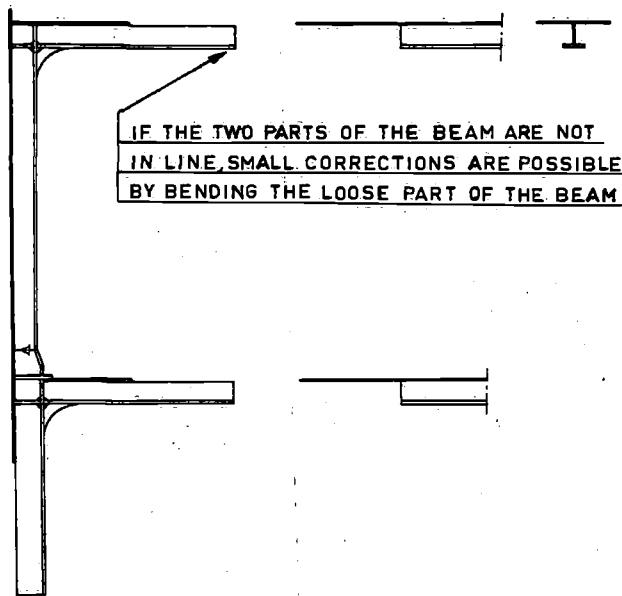


Fig. 1

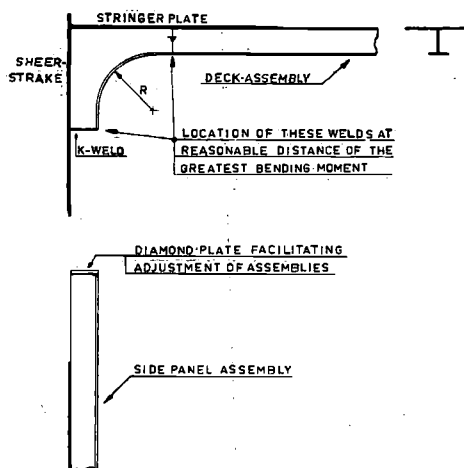


Fig. 2

became a welded construction instead of a riveted one. The construction is difficult to analyse mathematically and approximate stress calculations only give scanty information about what happens in reality. The strength calculations of these structural parts consist to an exceptional degree of hypothesis and approximation. This is due to:

- Imperfect knowledge about the applied loads
- Approximations in the strength theory
- Idealisation and schematization of the material used (assumed isotropic etc.)
- Complexity of the mathematical tool used.

All these difficulties together point to making tests and experiments, rather than to attack the problem purely scientifically. But, assuming experimental investigation, one must keep in mind, that

laboratory conditions are often very different from the reality existing on board ship. Even when trying to reproduce the latter as exactly as possible by making full scale models of the investigated structural members, the difference existing between the application of the loads in both cases and in the border conditions, will influence considerably the interpretation given to the test results. These influences are put forward in [2] and [3], giving a warning to experimentators when they apply laboratory-experiments to the real construction. They are especially important if scale effects in model tests are introduced also. Now model tests in ship structure research are often inevitable and extreme prudence in interpreting this sort of tests is indicated.

Another uncertainty comes from the interpretation of dynamic effects by means of static tests. Several times people have tried to explain the behaviour of dynamically loaded structures by static tests like *de Garmo* [4] for hatchcorners and *Irwin and Campbell* [5] for the intersection of longitudinals and oil-tight bulkheads in tankers. In both cases it must be considered very problematical whether the static strength obtained in the laboratory can be compared to the strength under the dynamic loads existing aboard ship.

The continuing use of static tests, even when they are not representative for the problem one wants to solve, results from the fact that, until recently, it was very difficult to execute dynamic tests, especially on a large scale. At the same time experimentators often underrate the risks they incur, when introducing dynamic conclusions from static results.

A simple static traction test with a structure gives us:

- the flow limit
- the breaking load
- the load corresponding to a limit of deformation or degree of plasticity
- the absorbed energy in the cases a, b and c.

Now, a ship's structure might be judged on one of these four criteria. But even supposing that they are valid, it will be quite a job to decide on which of these four our appreciation must be based, if we have to do with other loads than pure traction. Furthermore, if the construction has discontinuities, differences in stress will be great and the stress-concentrations will have to be taken into consideration. If the load is not a static one, but dynamic, it is next to impossible to decide which criterium is valid.

Stress-concentrations occur at abrupt changes of the section of the loaded beam. It is not always possible to avoid stress-concentrations [6], and the complex patterns of stress, which exist in places where these concentrations occur, oblige us to study

very carefully indeed the circumstances in which they have an effect.

The influence of these complex stresses on the strength of a structure depends on the type of loading (static or dynamic).

This shows the necessity:

- a. of making dynamic tests
- b. of making as much use as possible of full-scale models
- c. of making the models mentioned in b), so that they are simplified, schematized and idealized in such a way, that the verification of the tests may be possible by mathematical approximations.

But research on ship's structural members, such as beam-knees for instance, must give the biggest correspondence possible between the test-conditions and the real ship's conditions. Calculations must be as general as possible, in order to limit the number of test-pieces for one type of special subject.

In the case studied in this report, viz. beam-knees and other bracketed connections, tests were begun with idealized knees; after that intermediate constructions were investigated and finally some real knee-constructions as they are used nowadays on board ship. The intermediate and the definite forms are constantly compared to the corresponding idealized form. Only thus will the results be dependable and will they give information that can be applied to the actual loaded construction.

§ 2. Previous work executed in other countries carried out to investigate bracketed connections

There are two categories of bracketed connections:

- I. Bracketed connections in buildings, called hooks or angles.
- II. Bracketed connections in ships, generally called knees.

Tests on category I) are described in [7], [8] and [9].

Figure 3, published in [10] gives an idea of the most common hooks. In all these tests no wide flange-plates were connected to the orthogonal beams (no hull or deck-plates were present). The hooks were statically loaded (see fig. 3^a). All experiments compared only orthogonally connected beams without brackets, except that there were some models with special features (fig. 3^e and 3^h) or curved inner-flanges (fig. 3ⁱ, 3^j and 3^k).

Some conclusions from these tests on hooks were:

- a. The collapse *moment* of a bracketless orthogonal connection between two beams is about equal to the maximum bending moment that the smallest of the two beams can support.

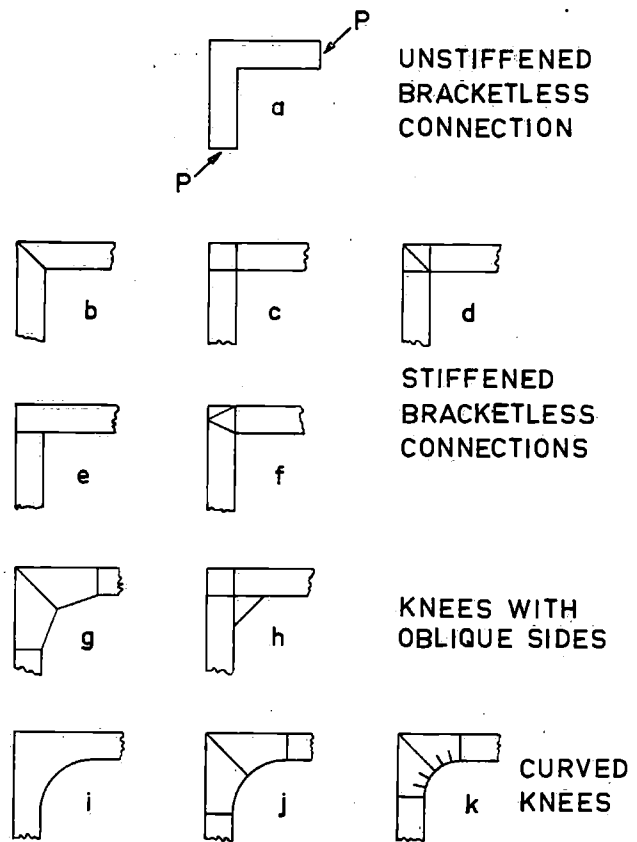


Fig. 3. Knee joints for welded rigid frames

- b. The plastic deformation before the collapse is then great.
- c. The collapse *load* is greater with bracketed connections than with orthogonally butt welded beams.
- d. Curved knees are better than square knees.
- e. With knees the plastic deformation remains small.
- f. Knees must therefore be used if plastic deformation is not acceptable.

Tests on category II.) are described in [11], [12] and [13]. *Haigh* [13] says that orthogonally butt welded beams without knees may be as strong as bracketed connections. *Kerkhof* [11] says the same.

That a complete set of tests is executed and why, is described in §1. Till now no dynamic tests with knees and other bracketed connections have been made, and the above mentioned recommendations for butt welded beams are not founded on serious dynamic considerations. In our tests the influence of stress concentrations is investigated, especially in regard to the role they play with dynamic loads.

As great plastic deformations are not allowed in ship's structures, it was necessary to investigate thoroughly the orthogonally butt welded connection without knees.

- c. Dynamic traction test with the maximum traction load as obtained by b).
- d. Stopping this dynamic traction test at the moment of the appearance of the first crack.
- e. Static compression test to beyond the elastic limit (see fig. 32).
- f. Dynamic compression test with the maximum compression load as obtained by e).
- g. Stopping this dynamic compression test at the moment of the appearance of the second (compression) crack.
- h. Static loading of the knee till the collapse under compression.

For some knees other dynamic loads, with a different mean load than that described in § 8, were applied.

The "idealization" of the curved knee-type (fig. 4) was obtained on the following bases: (Ideal knees)

1. The perpendicular flanges of the bracketed connection have a plate breadth equal to the frame-spacing.
2. The beam and the frame both have a symmetrical section. Both the interior flanges are connected to the curved prolongation of these flanges.
3. The construction is symmetrical to the diagonal parting under 45° from the corner formed by the beam and the frame.
4. There are butt welded joints between the knee and the beam and the knee and the frame. Two test-pieces (Nos. 12 and 13) were made out of one piece of plate as the coaming plate of knee, beam and frame. This was for comparison to the ordinary construction. The flanges of model No. 13 only have $\frac{1}{10}$ th of the breadth of the other (normal) flanges.
5. To eliminate internal stresses all knees, except No. 8, are annealed.
6. As verification by calculation must be possible, test-piece No. 13 was made. In general the ideal knee must serve as a standard of comparison for the other forms.
7. The dimensions of all knees were chosen in such a way, that comparison with the knees (scale 1 : 2) tested by the Norwegians in 1955 [12] was possible.
8. To obtain an indication about welding-influence, 9 out of the 13 ideal knees were normally welded. Nos. 10, 11, 12 and 13 were welded with special care. This special care consisted of radiographic inspection, repairing welding faults and not paying the welder at piece-work rates.

The triangular knee-type (see fig. 4) was designed on the following bases:

1. The sections at the break between beam, knee and frame must remain as much alike as possible.
2. The inner flanges of the knees are straight and form an angle of 135° with the flanges of the frame and the beam.
3. There are four different knees. Two have a symmetrical section in T-form, two have an unsymmetrical section in L-form. At each type of T- or L-form knee there is one of form A without tripping bracket and one of form B with tripping bracket (see table No. I).

Table I resumes the static and dynamic tests executed on all test-pieces. The indications are clearly put in this table and only a few remarks are necessary.

The triangular knee flanges have a tendency to twist and to trip in a plane perpendicular to the knee. Therefore in this case one has to distinguish primary and secondary bending stresses.

Moreover the flanges at the break of this type of knee are less resistant. Therefore form B is built up with tripping brackets to investigate this point. Such tripping brackets may be designed very advantageously in a good construction. It was found however, that under dynamic loads these tripping brackets are only effective when welded with K-welds (form B'; see table I). The common execution with fillet-welds gave no effective help to the knee, and there were even more cracks in form B than in form A.

For the "real-knees" there were introduced two orthogonally butt welded joints without knee-plates, one of T-type and one of L-type (electrodes: Smit-Conarc 49). All the other "real-knees" were with knee-plates (see fig. 4) (electrodes: Nekef OK. 48). The test-pieces Nos. 41, 42 and 43 are overlapping constructions, still much in use in naval architecture for mounting sections of the ship (see § 1). Test-piece No. 41' is obtained by milling away the welded stiffener of No. 41. Test-pieces 44-49 are different constructions used to this day.

It will be evident from table I, that not all the points a) to h) of the scope could be realized in every test-piece.

§ 4. Strain measurement and method of loading

An *Amsler* pulsator of 100 tons is used for the loading of the test-pieces. This pulsator, placed in the Ship Structure Laboratory of the Technological University of Delft, is described in [14], and a general view of the machine, measuring apparatus and testpiece is given in figure 5. The traction and compression test set-up is given in figure 5^a.

TABLE I

1 2		3		4 5 6		7 8 9		10		11 12		13		14	
TYPE	ITEM	SUBDIVISION		STATIC STRAINING AND STRESS DISTRIBUTION	TENSION	COMPRESSION	LOAD IN TONS	STATIC LOAD OF COLLAPSE	LOAD OF COLLAPSE	STATIC LOAD OF COLLAPSE	RESULTS AT CRACK INITIATION	RESULTS AT CRACK INITIATION	OBSERVATIONS	ITEM	
				ELASTIC STRAINING AND STRESS DISTRIBUTION	TENSION	COMPRESSION	LOAD IN TONS	LOAD OF COLLAPSE	LOAD OF COLLAPSE	LOAD OF COLLAPSE	LOAD OF COLLAPSE	LOAD OF COLLAPSE			
	1			●	●	●	18	>315	>315	>315	706	706	CRACK IN Y-WELD	1	
	2			●	●	●	18	438	438	438	438	438		2	
	3			●	●	●	116	566	566	566	566	566		3	
	4			●	●	●	18	1204	1204	1204	1204	1204	CRACK IN CURVED FLANGE AT POINT OF MAXIMUM STRESS	4	
	5			●	●	●	18	20	20	20	20	20		5	
	6			●	●	●	18	-255	-255	-255	-255	-255	COMPRESSION TEST CARRIED OUT AFTER FORMATION OF A SMALL CRACK DURING TENSILE FAILURE TEST	6	
	7			●	●	●	18	5	5	5	5	5		7	
	8			●	●	●	18	367	367	367	367	367	CRACK BETWEEN CURVED FLANGE AND WEB	8	
	9			●	●	●	18	>1570	>1570	>1570	>1570	>1570	CRACK IN Y-WELD	9	
	10			●	●	●	18	>500	>500	>500	>500	>500	FAILURE OUTSIDE OF TEST REGION	10	
	11			●	●	●	18	>910	>910	>910	>910	>910	AVERAGE LOAD GRADUALLY RAISED UNTIL FAILURE OCCURRED. AVERAGE LOAD AT FAILURE WAS 910 TONS	11	
	12			●	●	●	18	>910	>910	>910	>910	>910	FAILURE OUTSIDE OF TEST REGION	12	
	13			●	●	●	18	>910	>910	>910	>910	>910	EXCELLENT WELDING. STRESS RELIEVED	13	
	21a			●	●	●	18	>250	>250	>250	>250	>250	EXCELLENT WELDING. STRESS RELIEVED	21a	
	21b			●	●	●	18	>250	>250	>250	>250	>250	EXCELLENT WELDING. STRESS RELIEVED	21b	
	21c			●	●	●	18	>250	>250	>250	>250	>250	EXCELLENT WELDING. STRESS RELIEVED	21c	
	22a			●	●	●	18	105	105	105	105	105	DYNAMIC TEST CARRIED OUT AFTER STATIC TEST	22a	
	22b			●	●	●	18	>53	>53	>53	>53	>53	DYNAMIC TEST CARRIED OUT AFTER STATIC TEST	22b	
	22c			●	●	●	18	>53	>53	>53	>53	>53	DYNAMIC TEST CARRIED OUT AFTER STATIC TEST	22c	
	23a			●	●	●	18	212	212	212	212	212	COMPRESSION TEST CARRIED OUT AFTER TENSILE TEST	23a	
	23b			●	●	●	18	20	20	20	20	20	COMPRESSION TEST CARRIED OUT AFTER TENSILE TEST	23b	
	23c			●	●	●	18	9	9	9	9	9	COMPRESSION TEST CARRIED OUT AFTER TENSILE TEST	23c	
	216			●	●	●	18	>250	>250	>250	>250	>250	EXCELLENT WELDING. STRESS RELIEVED	216	
	217			●	●	●	18	>275	>275	>275	>275	>275	EXCELLENT WELDING. STRESS RELIEVED	217	
	218			●	●	●	18	95	95	95	95	95	EXCELLENT WELDING. STRESS RELIEVED	218	
	219			●	●	●	18	42	42	42	42	42	EXCELLENT WELDING. STRESS RELIEVED	219	
	220			●	●	●	18	192	192	192	192	192	EXCELLENT WELDING. STRESS RELIEVED	220	
	221			●	●	●	18	>100	>100	>100	>100	>100	EXCELLENT WELDING. STRESS RELIEVED	221	
	222			●	●	●	18	46	46	46	46	46	EXCELLENT WELDING. STRESS RELIEVED	222	
	223			●	●	●	18	14	14	14	14	14	EXCELLENT WELDING. STRESS RELIEVED	223	
	224			●	●	●	18	205	205	205	205	205	EXCELLENT WELDING. STRESS RELIEVED	224	
	225			●	●	●	18	27	27	27	27	27	EXCELLENT WELDING. STRESS RELIEVED	225	
	226			●	●	●	18	192	192	192	192	192	EXCELLENT WELDING. STRESS RELIEVED	226	
	227			●	●	●	18	>100	>100	>100	>100	>100	EXCELLENT WELDING. STRESS RELIEVED	227	
	228			●	●	●	18	46	46	46	46	46	EXCELLENT WELDING. STRESS RELIEVED	228	
	229			●	●	●	18	50	50	50	50	50	EXCELLENT WELDING. STRESS RELIEVED	229	
	230			●	●	●	18	>169	>169	>169	>169	>169	EXCELLENT WELDING. STRESS RELIEVED	230	
	231			●	●	●	18	>35	>35	>35	>35	>35	EXCELLENT WELDING. STRESS RELIEVED	231	
	232			●	●	●	18	>35	>35	>35	>35	>35	EXCELLENT WELDING. STRESS RELIEVED	232	
	233			●	●	●	18	>35	>35	>35	>35	>35	EXCELLENT WELDING. STRESS RELIEVED	233	
	234			●	●	●	18	>35	>35	>35	>35	>35	EXCELLENT WELDING. STRESS RELIEVED	234	
	235			●	●	●	18	>35	>35	>35	>35	>35	EXCELLENT WELDING. STRESS RELIEVED	235	
	236			●	●	●	18	>35	>35	>35	>35	>35	EXCELLENT WELDING. STRESS RELIEVED	236	
	237			●	●	●	18	>35	>35	>35	>35	>35	EXCELLENT WELDING. STRESS RELIEVED	237	
	238			●	●	●	18	>35	>35	>35	>35	>35	EXCELLENT WELDING. STRESS RELIEVED	238	
	239			●	●	●	18	>35	>35	>35	>35	>35	EXCELLENT WELDING. STRESS RELIEVED	239	
	240			●	●	●	18	>35	>35	>35	>35	>35	EXCELLENT WELDING. STRESS RELIEVED	240	
	241			●	●	●	18	>35	>35	>35	>35	>35	EXCELLENT WELDING. STRESS RELIEVED	241	
	242			●	●	●	18	>35	>35	>35	>35	>35	EXCELLENT WELDING. STRESS RELIEVED	242	
	243			●	●	●	18	>35	>35	>35	>35	>35	EXCELLENT WELDING. STRESS RELIEVED	243	
	244			●	●	●	18	>35	>35	>35	>35	>35	EXCELLENT WELDING. STRESS RELIEVED	244	
	245			●	●	●	18	>35	>35	>35	>35	>35	EXCELLENT WELDING. STRESS RELIEVED	245	
	246			●	●	●	18	>35	>35	>35	>35	>35	EXCELLENT WELDING. STRESS RELIEVED	246	
	247			●	●	●	18	>35	>35	>35	>35	>35	EXCELLENT WELDING. STRESS RELIEVED	247	
	248			●	●	●	18	>35	>35	>35	>35	>35	EXCELLENT WELDING. STRESS RELIEVED	248	
	249			●	●	●	18	>35	>35	>35	>35	>35	EXCELLENT WELDING. STRESS RELIEVED	249	
	250			●	●	●	18	>35	>35	>35	>35	>35	EXCELLENT WELDING. STRESS RELIEVED	250	
	251			●	●	●	18	>35	>35	>35	>35	>35	EXCELLENT WELDING. STRESS RELIEVED	251	
	252			●	●	●	18	>35	>35	>35	>35	>35	EXCELLENT WELDING. STRESS RELIEVED	252	
	253			●	●	●	18	>35	>35	>35	>35	>35	EXCELLENT WELDING. STRESS RELIEVED	253	
	254			●	●	●	18	>35	>35	>35	>35	>35	EXCELLENT WELDING. STRESS RELIEVED	254	
	255			●	●	●	18	>35	>35	>35	>35	>35	EXCELLENT WELDING. STRESS RELIEVED	255	
	256			●	●	●	18	>35	>35	>35	>35	>35	EXCELLENT WELDING. STRESS RELIEVED	256	
	257			●	●	●	18	>35	>35	>35	>35	>35	EXCELLENT WELDING. STRESS RELIEVED	257	
	258			●	●	●	18	>35	>35	>35	>35	>35	EXCELLENT WELDING. STRESS RELIEVED	258	
	259			●	●	●	18	>35	>35	>35	>35	>35	EXCELLENT WELDING. STRESS RELIEVED	259	
	260			●	●	●	18	>35	>35	>35	>35	>35	EXCELLENT WELDING. STRESS RELIEVED	260	
	261			●	●	●	18	>35	>35	>35	>35	>35	EXCELLENT WELDING. STRESS RELIEVED	261	
	262			●	●	●	18	>35	>35	>35	>35	>35	EXCELLENT WELDING. STRESS RELIEVED	262	
	263			●	●	●	18	>35	>35	>35	>35	>35	EXCELLENT WELDING. STRESS RELIEVED	263	
	264			●	●	●	18	>35	>35	>35	>35	>35	EXCELLENT WELDING. STRESS RELIEVED	264	
	265			●	●	●	18	>35	>35	>35	>35	>35	EXCELLENT WELDING. STRESS RELIEVED	265	
	266			●	●	●	18	>35	>35	>35	>35	>35	EXCELLENT WELDING. STRESS RELIEVED	266	
	267			●	●	●	18	>35	>35	>35	>35	>35	EXCELLENT WELDING. STRESS RELIEVED	267	
	268			●	●	●	18	>35	>35	>35	>35	>35	EXCELLENT WELDING. STRESS RELIEVED	268	
	269			●	●	●	18	>35	>35	>35	>35	>35	EXCELLENT WELDING. STRESS RELIEVED	269	
	270			●	●	●	18	>35	>35	>35	>35	>35	EXCELLENT WELDING. STRESS RELIEVED	270	
	271			●	●	●	18	>35	>35	>35	>35	>35	EXCELLENT WELDING. STRESS RELIEVED	271	
	272			●	●	●	18	>35	>35	>35	>35	>35	EXCELLENT WELDING. STRESS RELIEVED	272	
	273			●	●	●	18	>35	>35	>35	>35	>35	EXCELLENT WELDING. STRESS RELIEVED	273	
	274			●	●	●	18	>35	>35	>35	>35	>35	EXCELLENT WELDING. STRESS RELIEVED	274	
	275			●	●	●	18	>35	>35	>35	>35	>35	EXCELLENT WELDING. STRESS RELIEVED	275	
	276			●	●	●	18	>35	>35	>35	>35	>35	EXCELLENT WELDING. STRESS RELIEVED	276	
	277			●	●	●	18	>35	>35	>35	>35	>35	EXCELLENT WELDING. STRESS RELIEVED	277	
	278			●	●	●	18	>35	>35	>35	>35	>35	EXCELLENT WELDING. STRESS RELIEVED	278	
	279			●	●	●	18	>35	>35	>35	>35	>35	EXCELLENT WELDING. STRESS RELIEVED	279	
	280			●	●	●	18	>35	>35	>35	>35	>35	EXCELLENT WELDING. STRESS RELIEVED	280	
	281			●	●	●	18	>35	>35	>35					

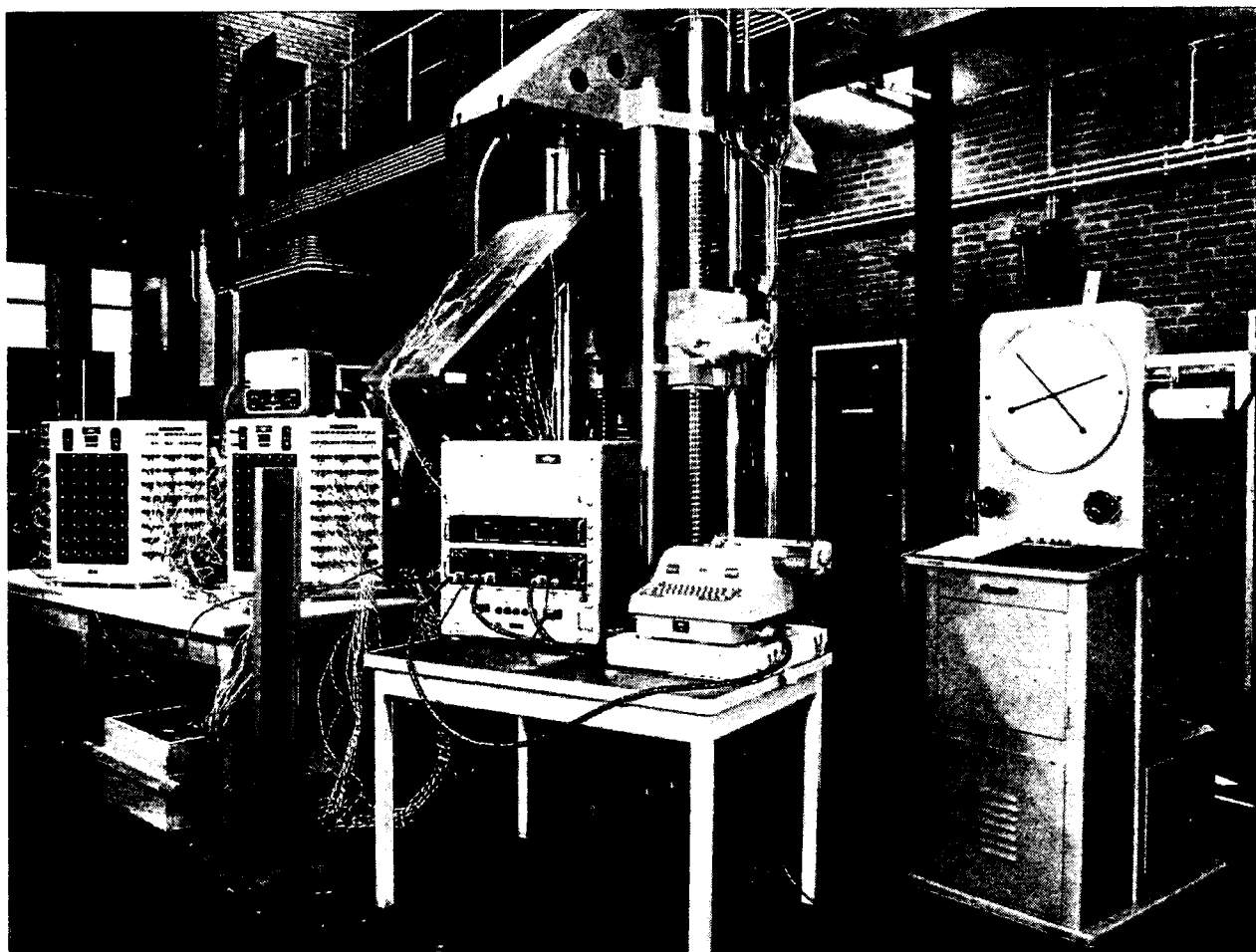


Fig. 5

The precision of the loads, both for the static tests and for the dynamic tests, is of the order of $\frac{1}{2}$ %.

The electronical measuring apparatus consists of *Philips* strain gauges, short base (type P.R. 9214 or P.R. 9218; $l = 4$ mm; $R = 120 \Omega$), of straight form or rosette-form.

For static measurement direct current is used. The strain gauges are mounted in a bridge of

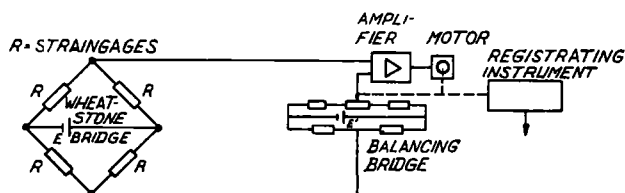


Fig. 6

Wheatstone (see fig. 6). The output voltage is compared to the voltage of a second bridge, which is fed separately. This difference of tension is amplified and an amplifier feeds an electric motor, which steers a potentiometer, so that the voltage of both bridges is equalized. The indication on the potentiometer gives the measurement of the strain of the construction at the place where the strain-gauge concerned is attached.

Figure 5 shows the pulsator with a full-scale knee in it. To the right a pendulum-manometer gives the indication of the applied load. The two boxes, shown on the left, are distributors to 48 strain-gauges each. They also contain the relays for the programme fixed beforehand for the measurements. One after the other these measurements are transmitted to the measuring box, shown in the middle in front of the pulsator. In this box are

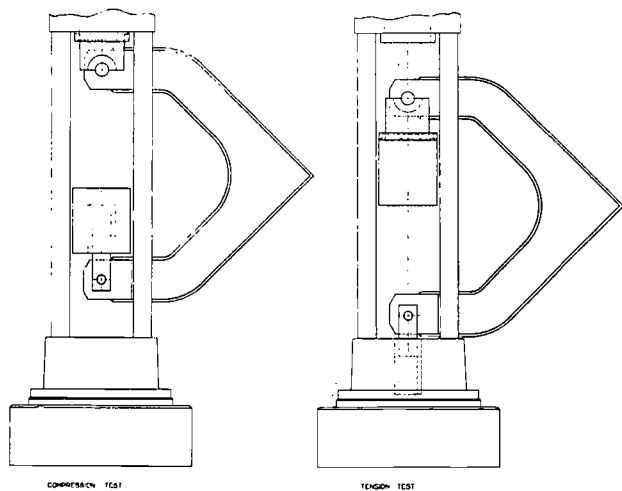


Fig. 5a. Specimens in test engine

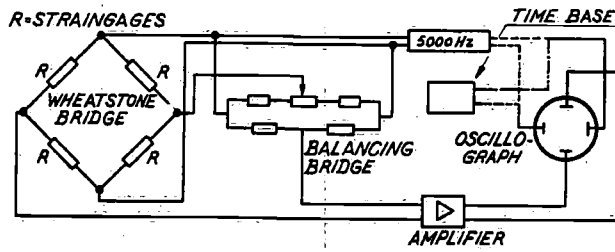


Fig. 7

the bridges of *Wheatstone*, which set to work the codification apparatus. On the box a luminous panel directly indicates the strain measured from the strain-gauge concerned. It is also possible to connect these indications with a type-writer, to the right of the box, which gives the measurement in writing for each point measured. In this way 2×48 points = 96 measurements are taken and recorded in writing in 10 minutes.

For dynamic measuring six measuring-points are taken. In this case the strain-gauges and the auxiliary bridge of *Wheatstone* are fed with a carrier current of 5000 Hz/4 V. The electrical scheme for this outfit is shown in figure 7. By means of a drag-resistance, the equilibrium between the two bridges of *Wheatstone* is realized so, that the input voltage of the potentiometer is zero at the moment that the load in the construction is minimum. The output voltage feeds the vertical plates in an oscillograph. The carrier current is connected to the horizontal plates (*Roberts method*) or a time indicator is connected to them (*Fink method*). Afterwards, the resistance-contact is placed in such a way, that the input voltage of the potentiometer is zero at the moment that the load in the construction is maximum. The distance between the places of the contacts of the drag-resistance is a measure of the amplitude of the load. In this way a dynamic effect is measured by a zero-method.

§ 5. The elastic distribution of strains and stresses

On one specimen of each type are placed a great number of strain-gauges and strain-rosettes of the *Philips* type mentioned above. The rosettes are placed on the coating plates of the test-piece, indicating the strains in this plate. Where possible, the strain-gauges are placed on both sides of the plate, in order to obtain the strains in the middle-plane of this plate. Where strains are measured in two directions, the stresses are calculated by the formula (see fig. 8):

$$\sigma_1 = \frac{m^2}{m^2-1} (E\varepsilon_1 + \frac{E\varepsilon_2}{m})$$

$$\sigma_2 = \frac{m^2}{m^2-1} (E\varepsilon_2 + \frac{E\varepsilon_1}{m})$$

- where ε_1 and ε_2 = measured strains
- σ_1 and σ_2 = calculated stresses in kg/cm²
- m = Poisson coefficient = 3,6
- E = Young's modulus = $2,1 \times 10^6$ kg/cm²

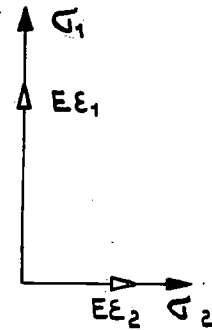


Fig. 8

The elastic measurements obtained are related to a supposed traction of 1 ton. The strains are given by $E\varepsilon$, the stresses by kg/cm². In this way $\sigma = 440$ kg/cm² is indicated by a linear local elastic deformation per ton of $440 E\varepsilon$.

The results of the rosette-measurements for the

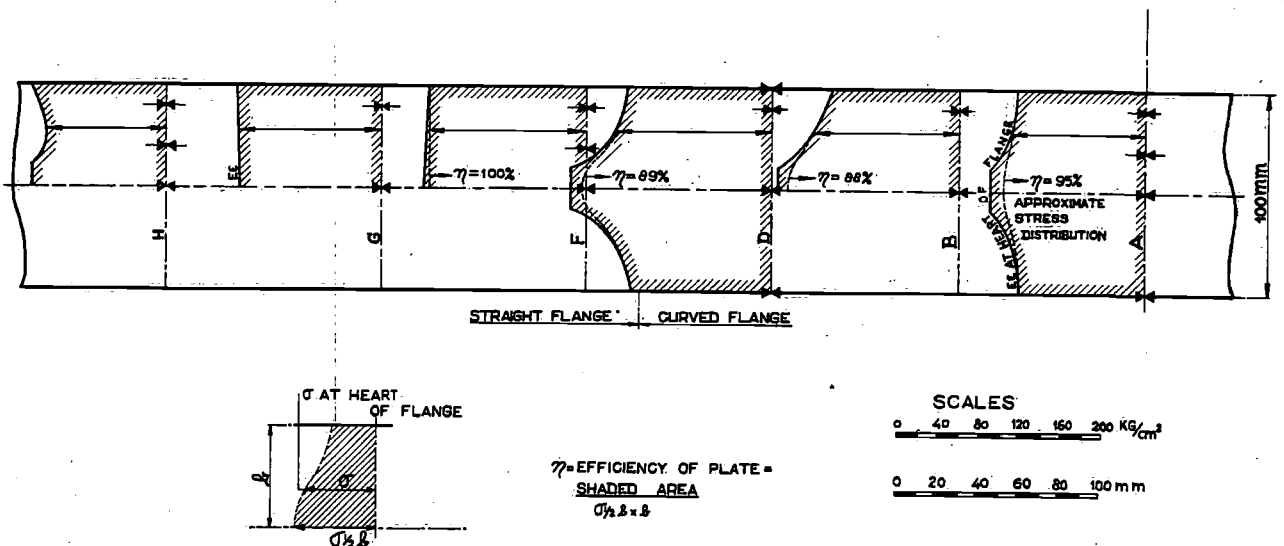


Fig. 9. Stresses at inner flange of ideal structure

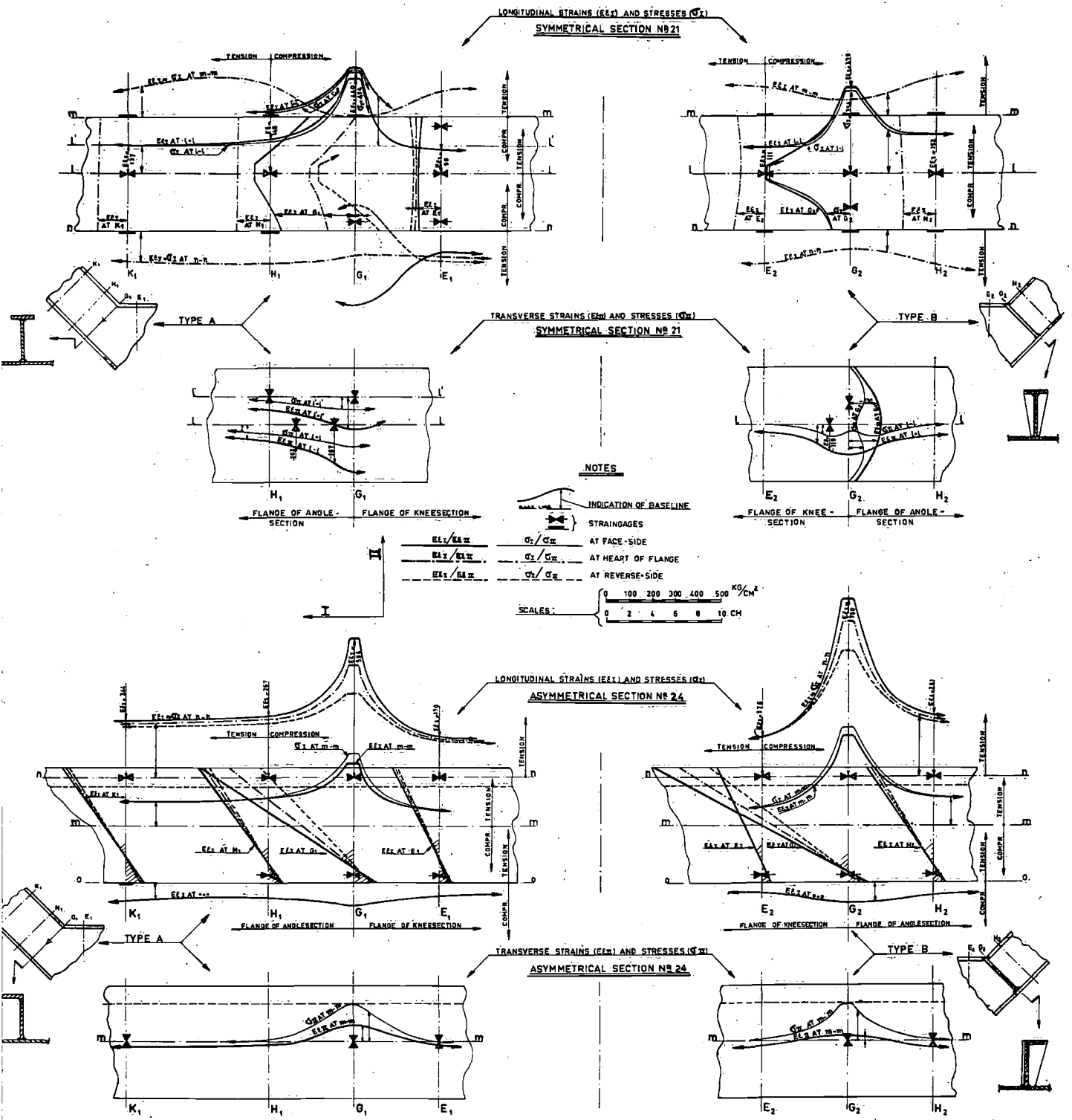


Fig. 10. Strain- and stress distribution at junction of flanges of triangular structures no. 21 and 24

coaming plates are obtained by tracing the Mohr circles for each place. The stresses are calculated as indicated above.

The strain-measurements for the flanges are combined with those of the rosettes. The results are plotted as curves for the perpendicular and parallel sections of the beam, the knee and the frame. In this way the distribution of stress for the main

directions in the coaming plates of the different test-pieces can be indicated and may be compared to each other. The distribution in the coaming plates is completed by indications of the main stresses measured by the rosettes and by cracked lacquered-isostatiques obtained on one test-piece.

The strain and stress distribution for the flanges of the ideal knees is given in figure 9. The efficiency

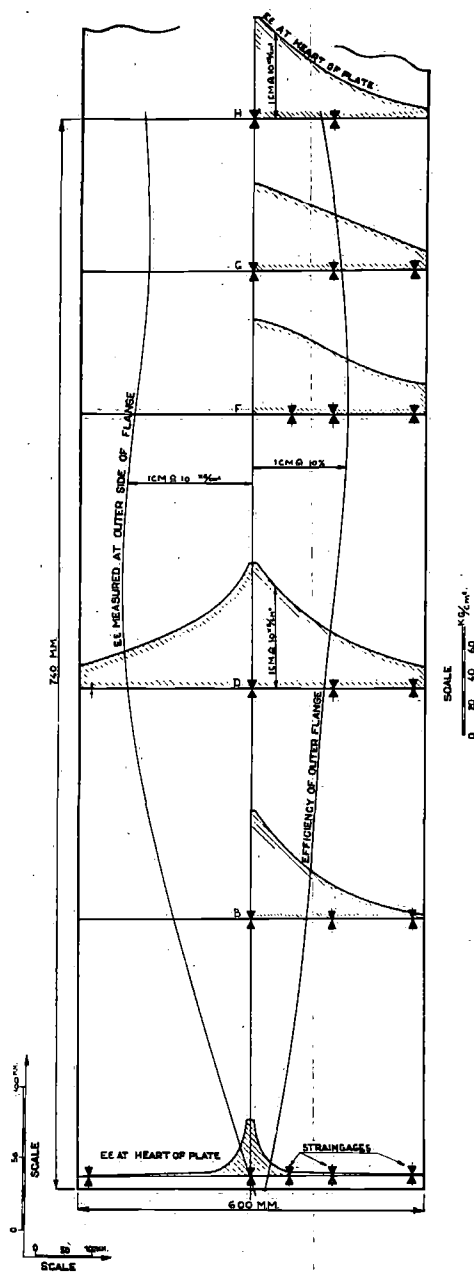


Fig. 11. Results of measurements at shell and deck flanges of ideal structure

of the curved flange is seen to be about 90 %. For the straight parts of the flange this amounts to 100 %.

Figure 10 indicates the same type of distribution for triangular knees.

Figure 11 indicates the strain-distribution in the middle of the hull-plate of the ideal knee. This distribution is also valid for the hull-plate of the triangular knee.

For both the ideal and the triangular knees, the test-results are indicated in the following figures:

Figure 12. Ideal knee; location of strain-gauges and principal stresses; trajectories of stress.

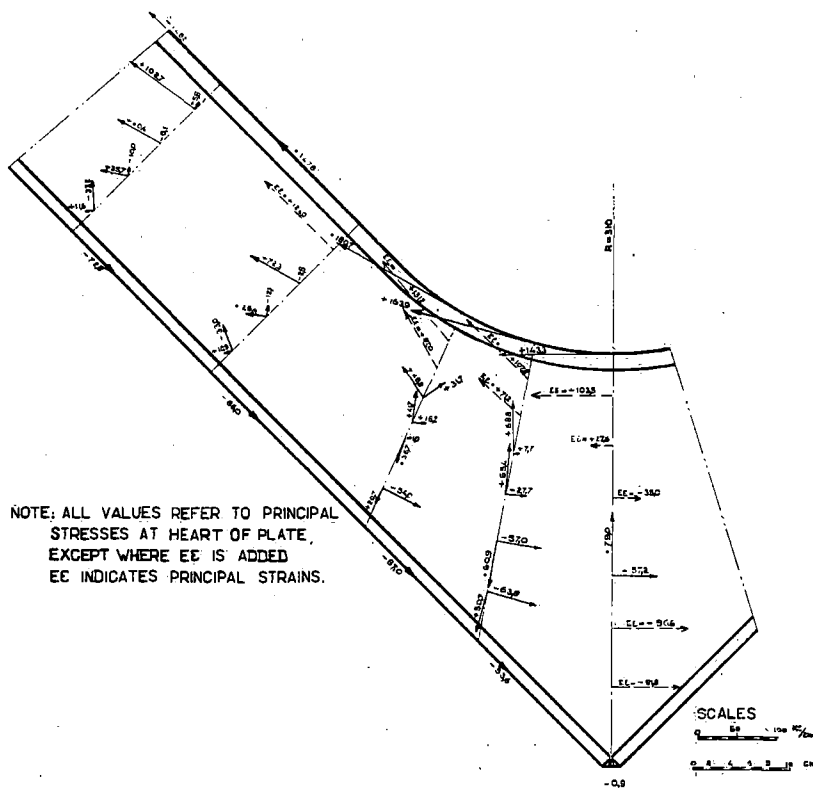


Fig. 12. Principal stresses of ideal structure

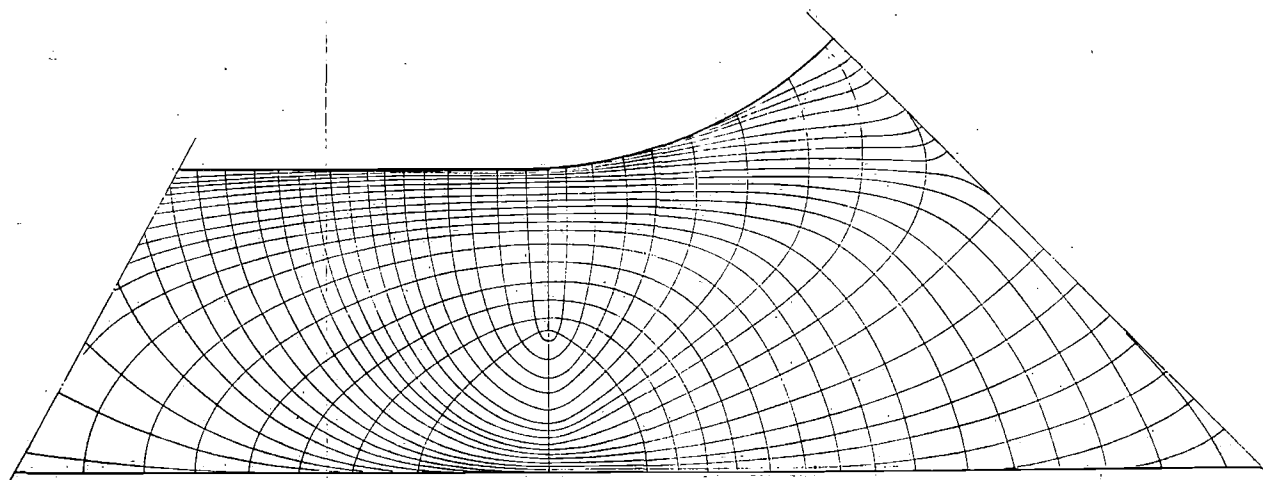


Fig. 12a. Trajectories of stress

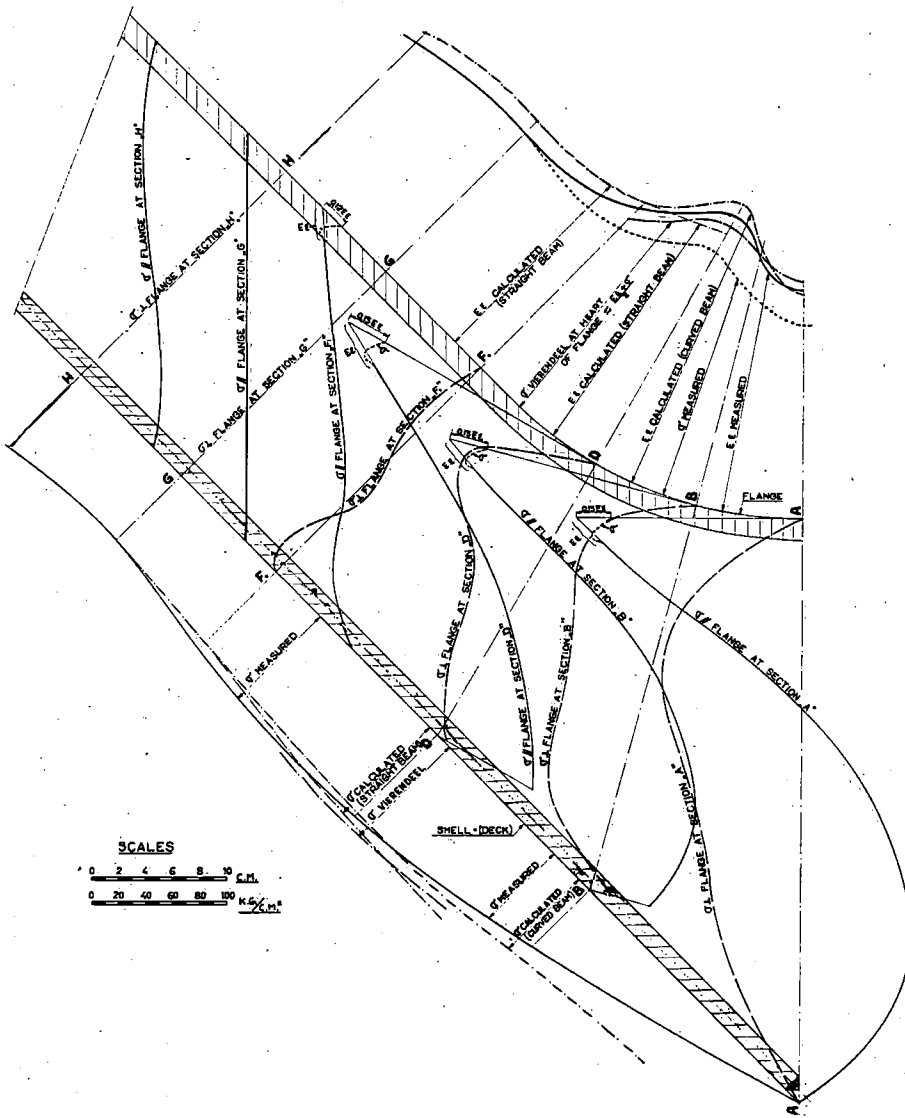


Fig. 13. Measured and calculated stresses in web of ideal structure no. 9

Figure 13. Ideal knee; stresses in beam, bracket and frame.

Figure 14. Ideal knee No. 13; stresses in beam, bracket and frame.

Figure 15. Symmetrical triangular knee; location of strain-gauges and principal stresses.

Figures 16 and 17. Symmetrical triangular knee; stresses in beam, bracket and frame.

Figure 18. Asymmetrical triangular knee; location of strain-gauges and principal stresses.

For the ideal knee (fig. 12 and 13) the section *H* is a control-section. In that place extra-sensitive strain-gauges are installed. It is seen that the strain-distribution follows a flat-S-curve and that *Navier's* law is not valid in this case. This is the result of "shear-lag" indicated and found to have influence also by *Opie* [1]. Although this phenomenon was not a part of the present investigation, it could not be avoided because of the very wide flanges of the specimens used. The internal moment calculated from this flat S-curve, was in correspondence with the moment due to the load of 1 ton. The stress

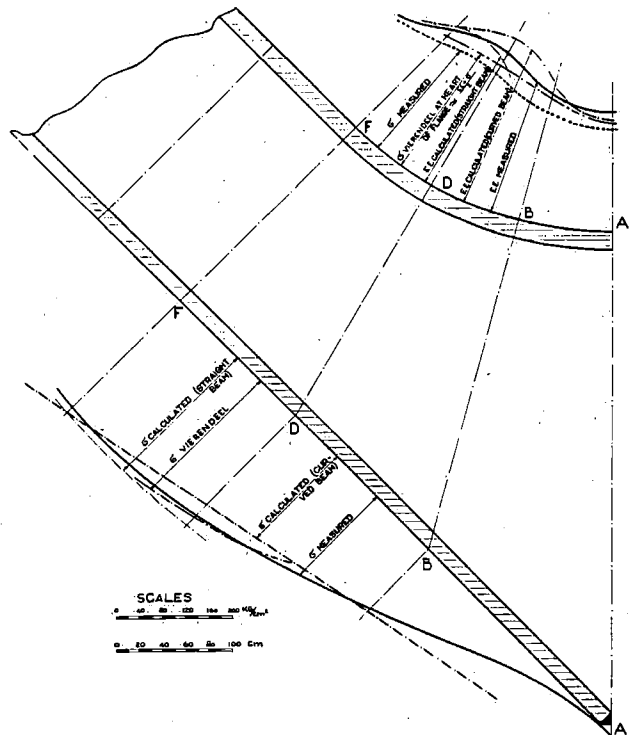


Fig. 14. Measured and calculated stresses at orthogonal and curved flanges of ideal structure no. 13

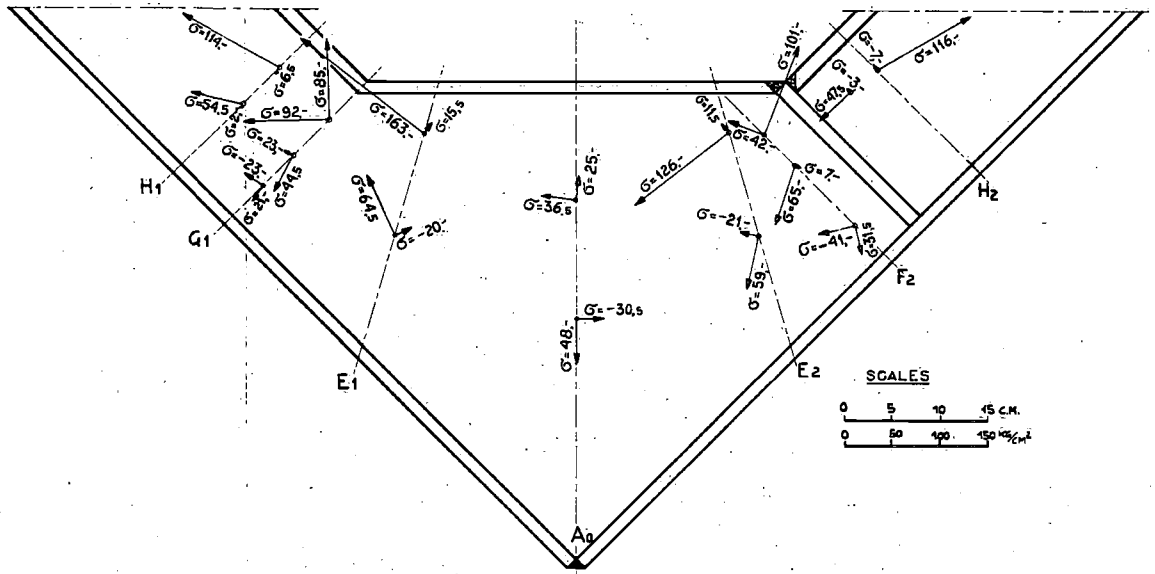


Fig. 15. Principal stresses at heart of plate of triangular bracket (symmetrical section)

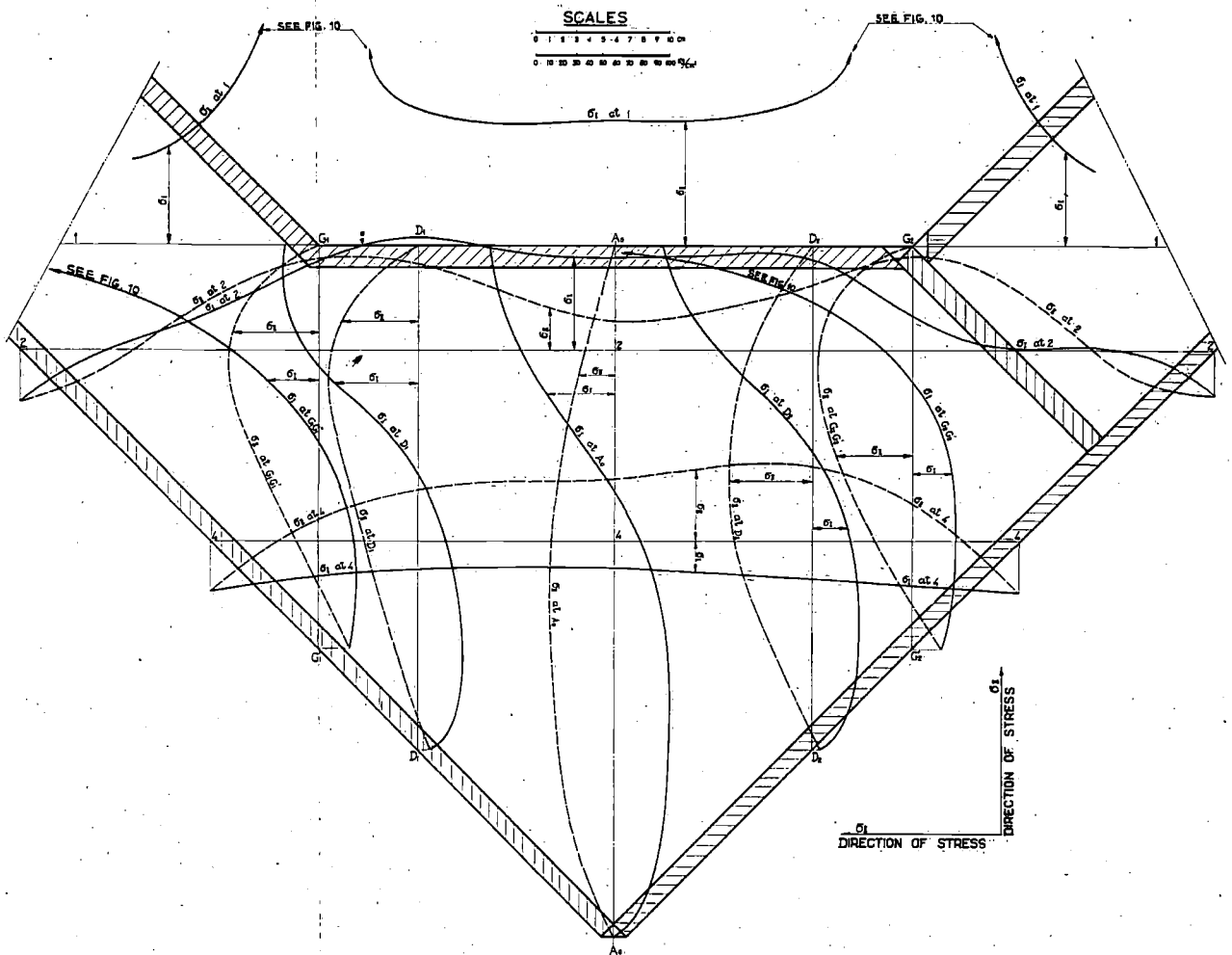


Fig. 16. Stresses in triangular bracket (symmetrical section)

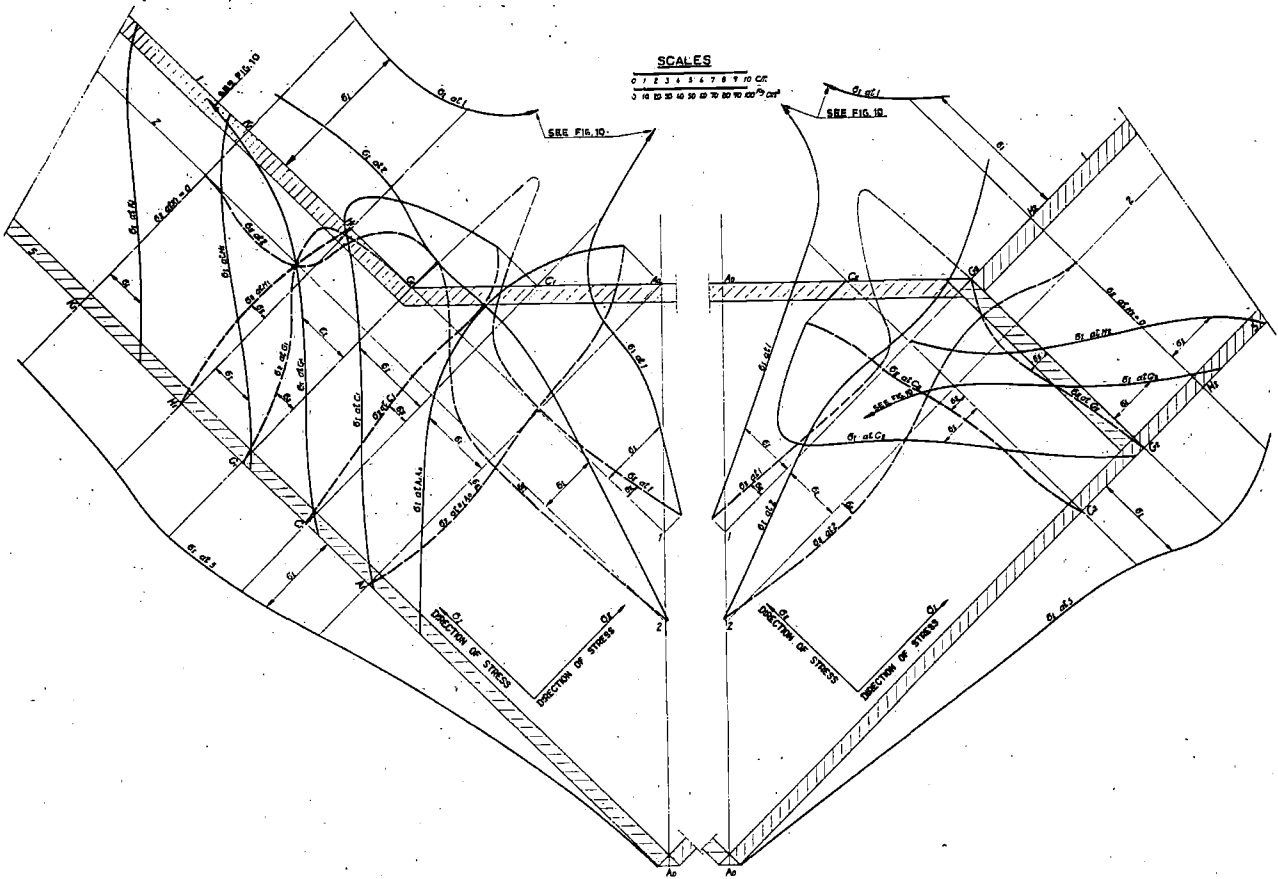


Fig. 17. Stresses in triangular bracket (symmetrical section)

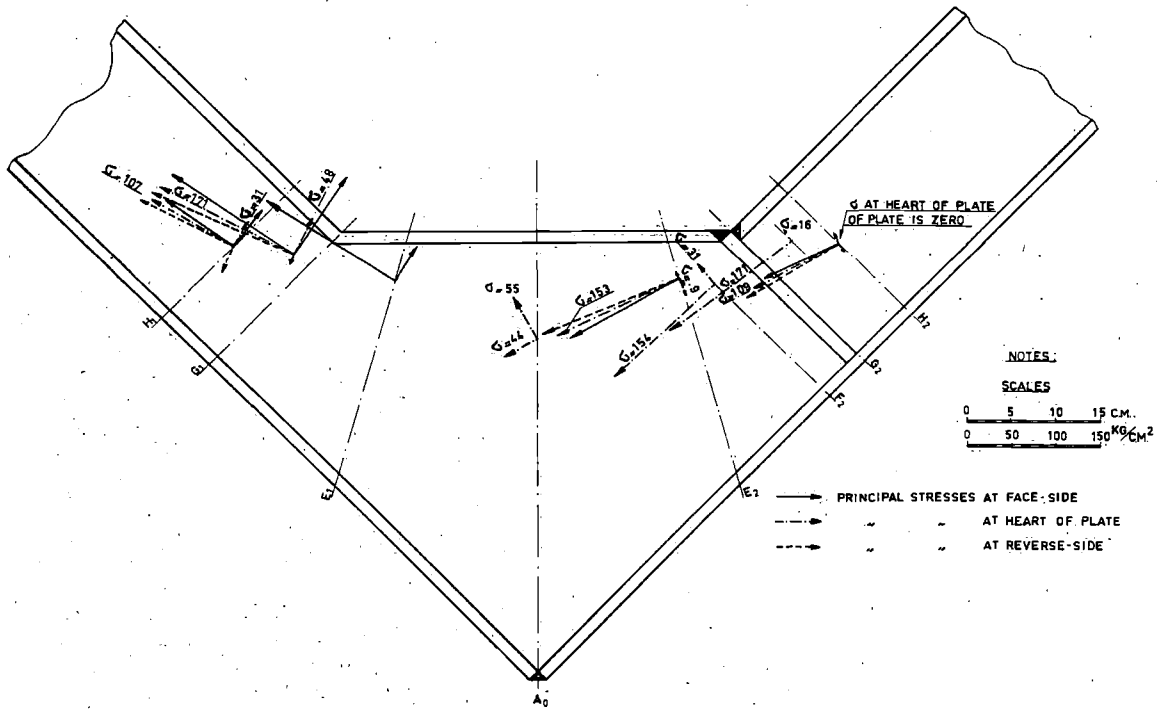


Fig. 18. Principal stresses in triangular bracket nr. 24 (asymmetrical section)

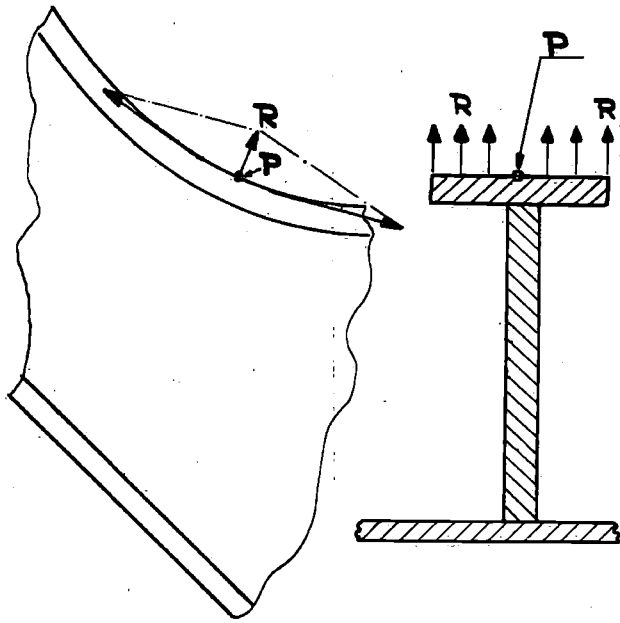


Fig. 19

as calculated from a linear distribution (*Navier's hypothesis*), taking into account the flange-efficiency, gave a value of 5 % higher than the measured one. This difference of 5 % is the result of "shear-lag". In section G, the stress distribution was quasi-linear.

The secondary bending has only an influence on the curved flanges. At the limits of these flanges perpendicular forces intervene with the curving of the flange of the ideal knee (see fig. 19). The measurements indicate that this secondary bending is appreciable. In the point P (fig. 19) compressive transverse forces cause a *Poisson effect*, which is responsible for a longitudinal strain in the flange at that point. Strain-gauges at that place give the total sum of the total bending-strain in P. The latter has been measured as being 14 %. So the primary bending-stress is about 14 % less than the strain-measurement $E\varepsilon$. In F the difference is still 12 %.

The stress indications in figure 13 take care of this phenomenon.

In the underside of the flange the magnitude of the stresses will be of the same order. Here three-dimensional stresses may become very dangerous. The tests have shown indeed that cracks originated especially at the weld connection between flange and coaming. This is confirmed by the dynamic tests (see § 8).

Generally speaking, the strain- and stress-distributions in the ideal knees are in good agreement with the calculations (see § 7 and appendix II). The bending stresses are greater in the flanges in D_1 (see fig. 12 and 13). The difference between these stresses and those in F is only 20 %. The con-

clusion can be that the ideal knee is behaving itself ideally.

Figure 10 shows the strains and stresses in the flanges of triangular knees. Apart from the breaks there is no reason to suppose a secondary bending. Therefore the flange-efficiency is considered to be 100 %.

The influence of tripping brackets on the stress-distribution and on the maximum stress in the flanges seems to be negligible (see fig. 10). That secondary bending is more important in ideal knees than in triangular ones in the break A is explained by the lateral stress-distribution as shown in figure 20.

Figures 16 and 17 show the stress-distributions parallel and perpendicular to the flanges in the coaming-plates of symmetrical triangular knees. The tripping bracket has the following influence:

a) Reduction by one third in the stress parallel to this bracket, near the flange (σ_{II} at point 2, fig. 16).

b) Negligible influence on the stress perpendicular to the flange (σ_{II} at point 2, fig. 17).

On the other hand, the influence of the break is most important in the flanges (σ_I at point 1). There extreme high stresses are found, diminishing however fast in the coaming-plate (σ_I at G_1 ; σ_I at G_2). The stress distribution at H_1 and H_2 also shows that the influence of the breaks gives way only to local stress-concentration.

The most remarkable result of these tests is the presence of large secondary stresses in the flanges of the asymmetrical triangular knees (see fig. 10).

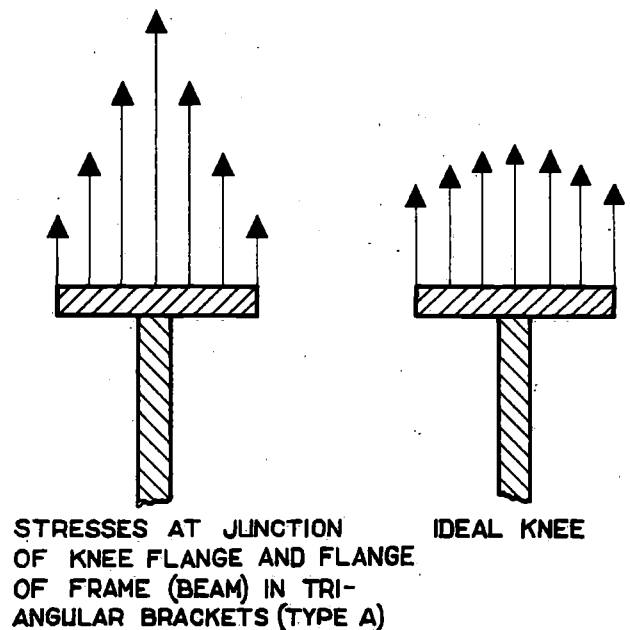
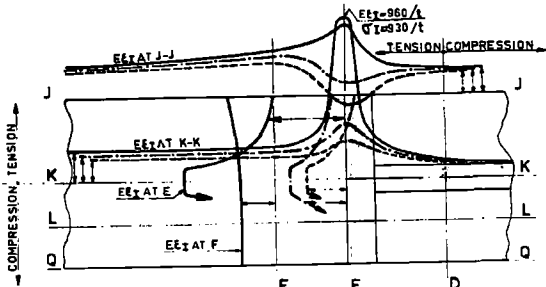
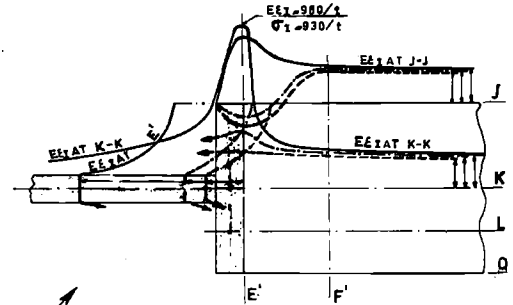


Fig. 20

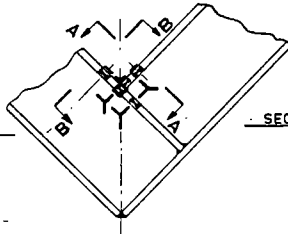
LONGITUDINAL STRAINS (ϵ_x) AT SECTION A-A
CONSTRUCTION NR 31



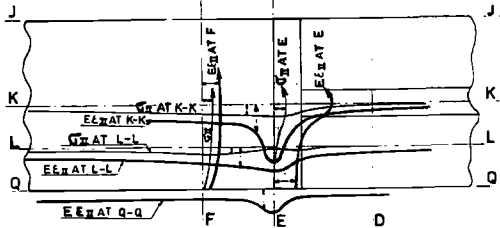
LONGITUDINAL STRAINS (ϵ_x) AT SECTION B-B
CONSTRUCTION NR 31



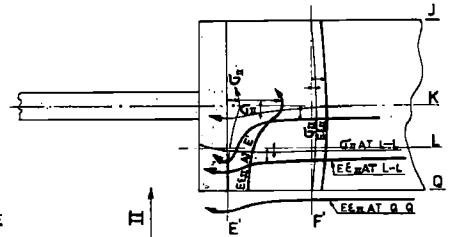
DISPOSITION OF STRAINGAGES
CONSTRUCTION NR 31



TRANSVERSE STRAINS (ϵ_y) AND STRESSES (σ_y)
AT SECTION A-A
CONSTRUCTION NR 31

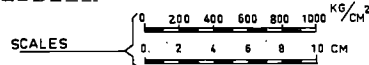


TRANSVERSE STRAINS (ϵ_y) AND STRESSES (σ_y)
AT SECTION B-B
CONSTRUCTION NR 31

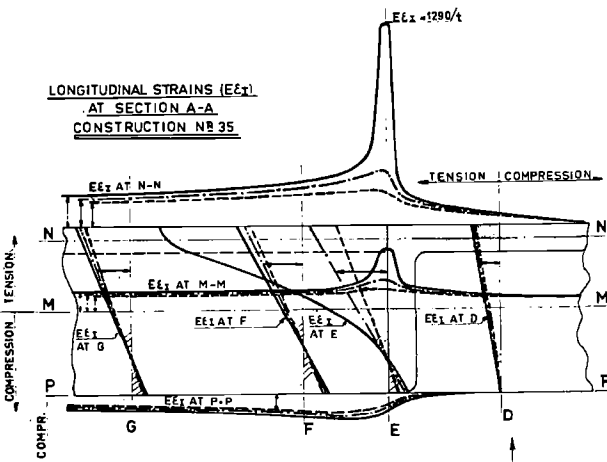


NOTES

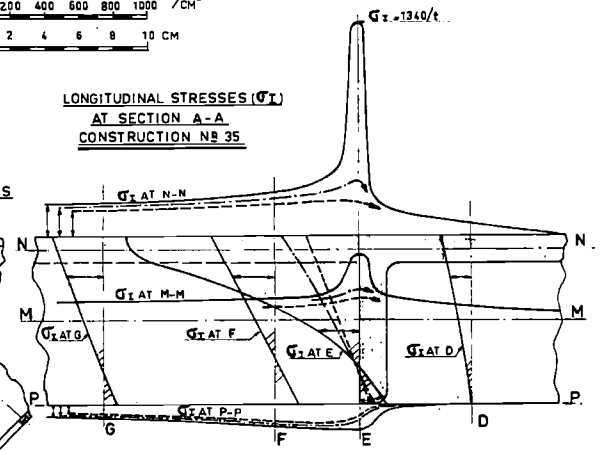
- INDICATION OF BASELINE
- STRAINGAGES
- σ_x σ_y AT FACE-SIDE
- σ_x σ_y AT HEART OF FLANGE
- σ_x σ_y AT REVERSE-SIDE



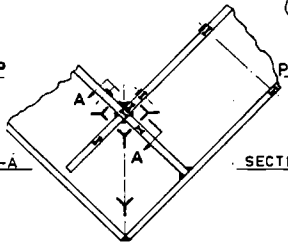
LONGITUDINAL STRAINS (ϵ_x)
AT SECTION A-A
CONSTRUCTION NR 35



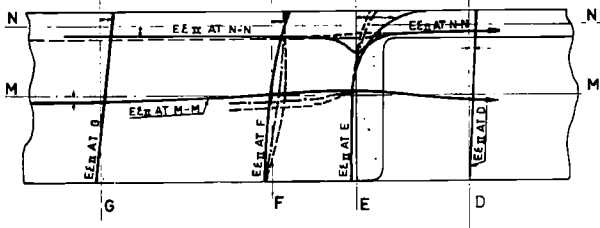
LONGITUDINAL STRESSES (σ_x)
AT SECTION A-A
CONSTRUCTION NR 35



DISPOSITION OF STRAINGAGES
CONSTRUCTION NR 35



TRANSVERSE STRAINS (ϵ_y) AT SECTION A-A
CONSTRUCTION NR 35



TRANSVERSE STRESSES (σ_y) AT SECTION A-A
CONSTRUCTION NR 35

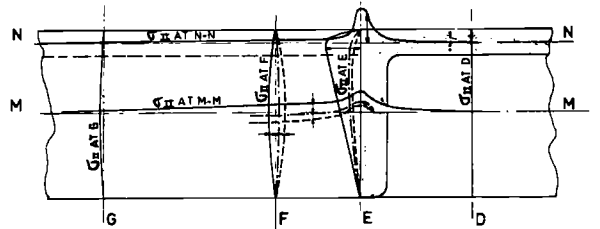


Fig. 21. Details of flanges at junction of bracketless constructions nr. 31 + 35

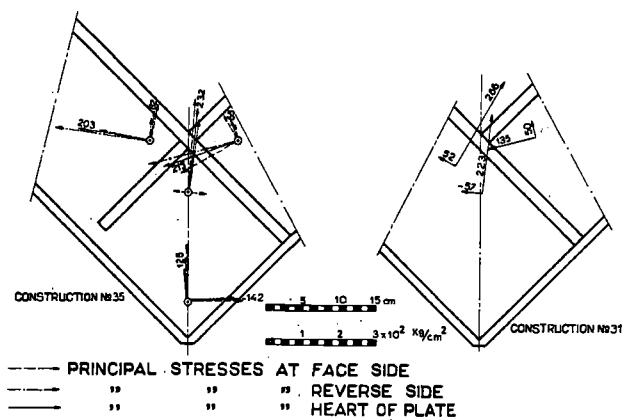


Fig. 22. Principal stresses in bracketless constructions

The asymmetric structure has a very different stress-distribution in the breadth of the flange, as compared to the symmetrical flange. The stresses at the root of the coaming-plate are up to twice as

high. At the limit of the flange there is almost no strain. The efficiency of this flange therefore can't be valued higher than 50 % (see fig. 10).

The results of these elastic stress- and strain-measurements for the real knees are treated at the end of this paragraph. For the three types mentioned (ideal knee, symmetrical triangular knee and asymmetrical triangular knee) the measurement *per ton load* is found as:

	Per ton load
Ideal knee	$\sigma_i = 180 \text{ kg/cm}^2$
Symmetrical triangular knee	
type A: $\sigma_{nA} = 413 \text{ kg/cm}^2$	$= 2.3 \sigma_i$
Symmetrical triangular knee	
type B: $\sigma_{nB} = 354 \text{ kg/cm}^2$	$= 2 \sigma_i$
Asymmetrical triangular knee	
type A: $\sigma_{nA} = 596 \text{ kg/cm}^2$	$= 3.3 \sigma_i = 1.4 \sigma_{nA}$
Asymmetrical triangular knee	
type B: $\sigma_{nB} = 780 \text{ kg/cm}^2$	$= 5.1 \sigma_i = 1.9 \sigma_{nB}$

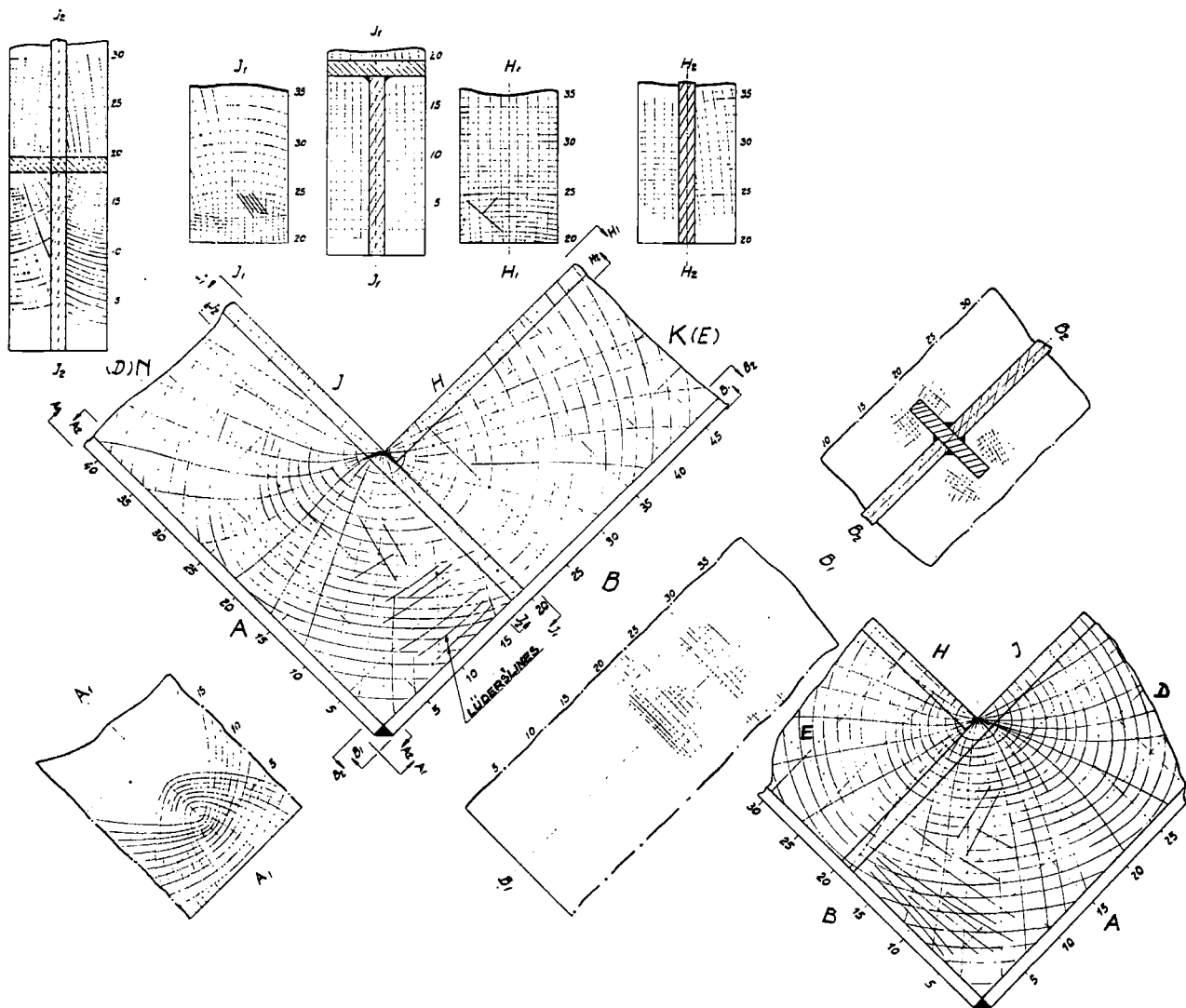


Fig. 23. Trajectories of stress (constr. nr. 31)

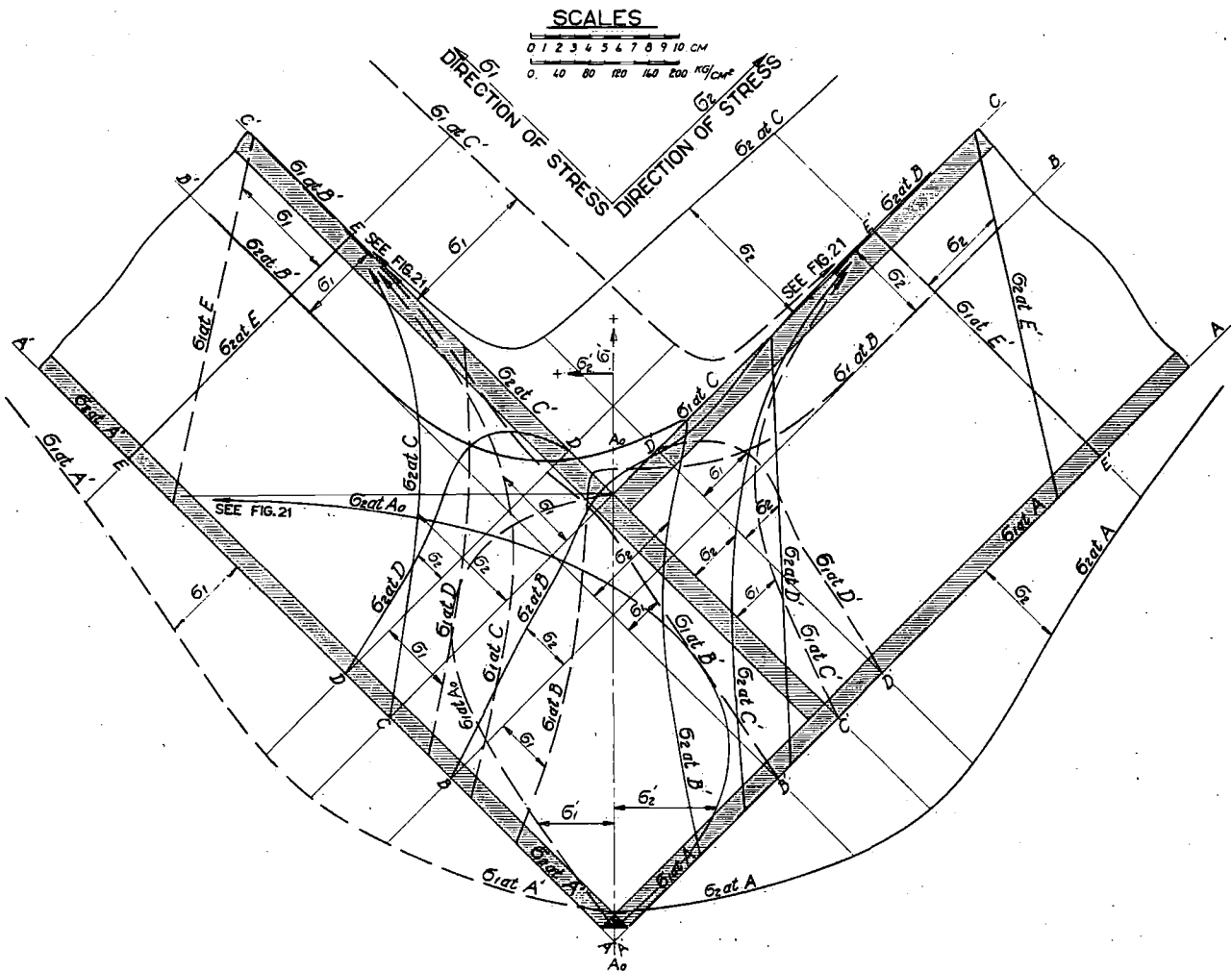


Fig. 24. Stresses in bracketless construction no. 31. (symmetrical section)

As the stress-distribution for the coaming plates of asymmetrical knees is nearly the same as for the symmetrical knees, the latter is not shown separately in a figure.

The results of the measurements at the orthogonally butt welded beams and frames without bracketplates are given in figures 21, 22, 23, 24 and 25. The profile (section) which goes through up to the corner, is called "frame".

Figure 21 shows first the symmetrical test-piece No. 31. The stress-distribution is given both along the flange of the frame and along the flange of the beam. For the asymmetrical test-piece where both the frame and the beam are continuous at the break, only the stress-distribution in the flange of the frame is shown in figure 21. The figure indicates, that for T-frames the secondary stresses σ_2 are small. This means that the beam-flanges only transmit very small forces to the frame-flanges. Nevertheless transverse bending deformation of the frame-flange in the direction of the beam is appreciable ($E\varepsilon_1$ at J). This is due to Poisson-contraction at the point of high primary stresses in the frame-flange ($\tau_1/\text{ton} = 930 \text{ kg/cm}^2$).

The continuation of the frame-flange after the crossing with the beam-flange is an amelioration of the construction (compare No. 35 with No. 31). The stress-concentration factors are:

$$k_{35} = 3.5 \text{ (L-section)}$$

$$k_{31} = 4.2 \text{ (T-section)}$$

and the maximum stresses become:

Test-piece No. 31, T-section:

$$930 \text{ kg/cm}^2 \text{ per ton load}$$

Test-piece No. 35, L-section:

$$1340 \text{ kg/cm}^2 \text{ per ton load}$$

Therefore it follows that the smaller flange-efficiency of the L-section (<50%) absorbs completely the advantage of the smaller stress-concentration factor. Thus, symmetrical sections for this orthogonally butt welded connection are preferable. Nevertheless figures 24 and 25 show, that the prolongation of the frame-flange reduces the stresses in the coaming-plate considerably (about 50%).

The lacquer-crack test shows that the direction of the principal stresses is not so much influenced by this construction (fig. 23).

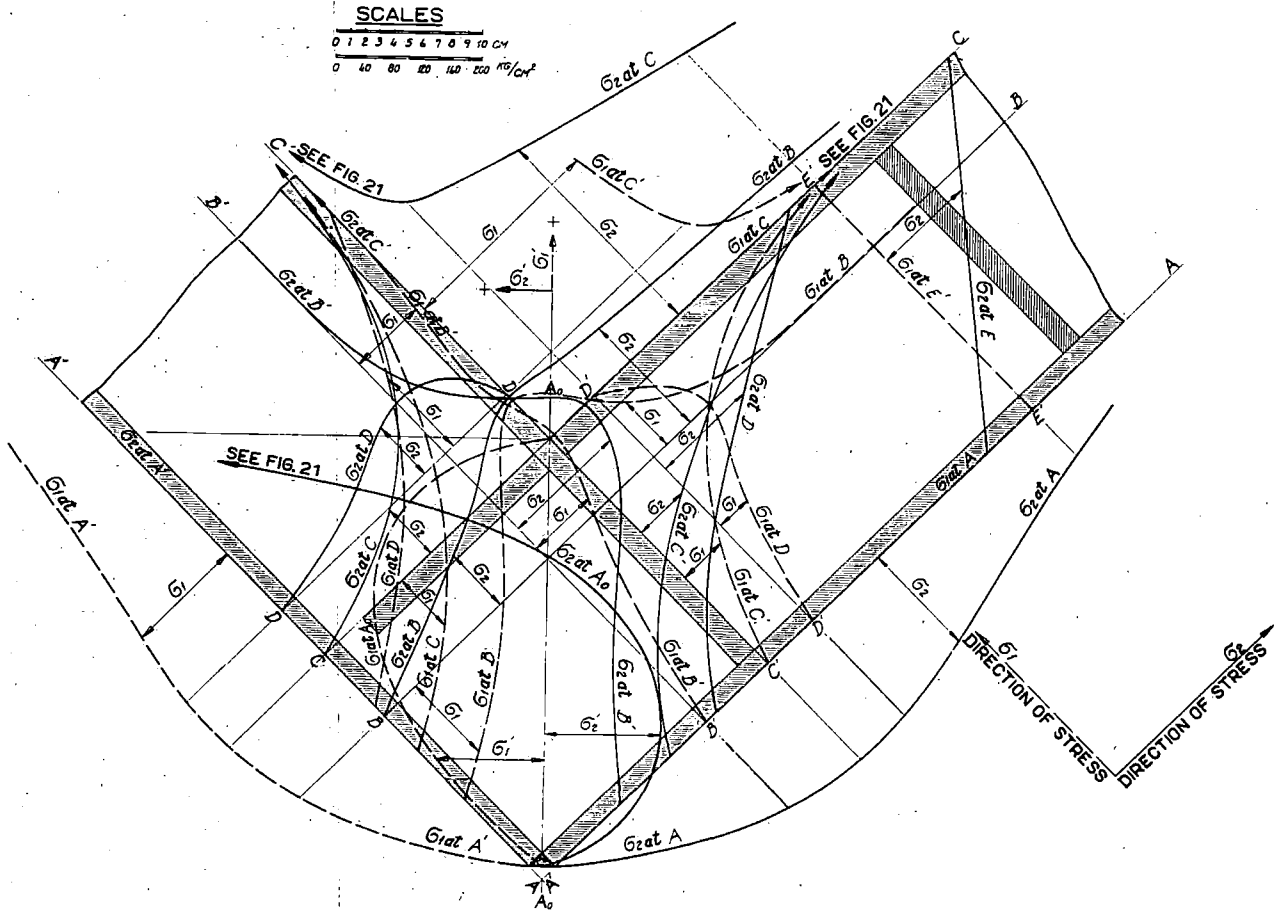


Fig. 25. Stresses at heart of web of asymmetrical construction no. 35

The results of the measurements of real knees are given in the figures 26, 27 and 28. These figures concern the test-pieces 41, 41', 44 and 47.

Test-piece No. 41 represents an old-fashioned welded construction, No. 44 and No. 47 are variations on this theme in order to obtain the influence of these variations.

The stresses at the border of the bracket are per ton load:

- Type 41 with bevelled border:
 σ at half length of the border: 158 kg/cm²
- Type 41' without bevelled border:
 σ at half length of the border: 189 kg/cm²
- Type 41 and 41' in the corner of the sections σ :
 250 kg/cm²
- Type 41, at the ends of the bevel σ :
 415 and 352 kg/cm²
- Type 44 along the rounded border σ :
 475 kg/cm²

From the point of view of elastic stresses it is sufficient to have a knee without bevelled border. Stress-concentration at the ends is then non-existent. The rounded knee has the disadvantage that too little material remains and the stresses increase. For this reason type 47 has been tested. However this

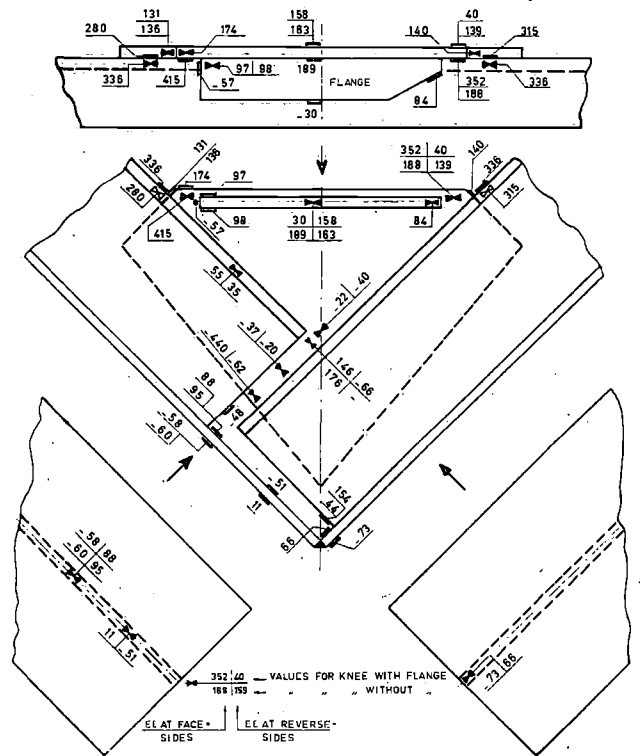


Fig. 26. Results of measurements in Eg per ton for construction nr. 41, with and without knee flange

knee with overlap on the beam is not recommended as local deflection perpendicular to the knee is possible (see fig. 28).

The stresses in beam and frame at the ends of the knee were:

Type 41, at 17 mm from the end of the knee:
 $\sigma = 336 \text{ kg/cm}^2$ per ton load
 (fig. 26)

Type 47, idem from the end of the rounded knee:
 $\sigma = 320 \text{ kg/cm}^2$ per ton load
 (fig. 28)

The stresses are measured at the flanges of the sections. Near this point the stresses in the rounded knee-plates are much lower than in the triangular ones (see fig. 26 and 28).

There are appreciable stresses in the knee between the end of the beam and the exterior flange of the frame (see test-pieces 41, 44 and 47). The disadvantage of type 41 lies in the lack of support of parts of the deckplate and the hullplate in the corner. The knee itself now becomes very highly loaded and the discontinuity of the connection adds to the difficulties. For instance:

Type 41*): σ in the unsupported part of the knee between beam and frame = $-440/-62 \text{ kg/cm}^2$

Type 44 : σ in the unsupported part of the knee between beam and frame = $258/105 \text{ kg/cm}^2$

Type 47 : σ in the unsupported part of the knee between beam and frame = $-310/240 \text{ kg/cm}^2$

Type 47 : σ in the extension of the beam-flange = $-364/640 \text{ kg/cm}^2$

Through the supplementary connection between frame and deck-plate the construction has become more stiff, but in the knee the local deflection has

*) Note: Data on the elastic stresses concerning analogous constructions such as type 41 with other knees and other plate thicknesses as well as other dimensions, are given in [12]. Appendix III gives some further information.

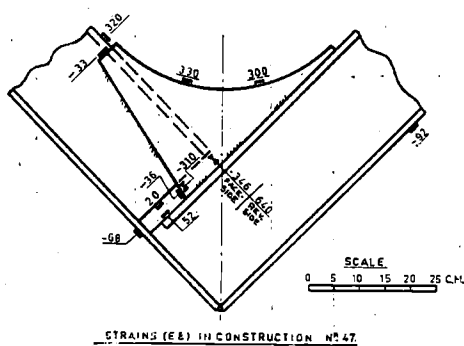


Fig. 28

become greater. Therefore knees with lighting-holes and bevelled flanges have been tested (see fig. 4, test-pieces 44' and 46'). The result has been that no amelioration was obtained (see figure 27). Neither did the lightening of the beam gives any result. The loss of rigidity of the beam reduced the moment ($P_1 + P_2$) (as shown in fig. 29). The presence of this moment explains the curious distribution of stresses at the notch-hole of test-piece 44. The deck-plate is very badly supported and deformation results as indicated in figure 29.

In table II, columns 1 to 5 give indications about the stress concentrations of all knees.

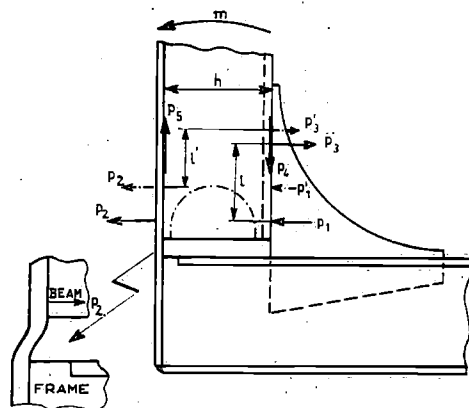


Fig. 29

§ 6. Traction tests till failure
 Compression tests till buckling

In most cases the traction-test till failure is not executed. In § 3 it has been stated that the load was applied till some plastic deformation occurred. The deformation-curves obtained in this way, are given in figure 30, the loads at which the elastic limit is reached in table II.

The compression loads resulting in collapse or buckling of the structure are also given in figure 30 and table II. The values of the flow limit in this case only are approximately true. Indeed the compression test was made after the traction test with the same test-piece, as described in § 3. So the Bauschinger effect comes into action and results in the disappearance of the flow limit. Therefore it is assumed that the real flow limit in compression is the same as in traction (table II). The inverted traction deformation-curves can thus partly be used as compression-deformation curves. The compression load is nearly independent of the way the tension load is applied before, as is shown by the test-pieces 6A, 11, 31, 34, 44 and 45.

The results of the compression tests are:

1. Types 31 and 35 have about the same structural value when the effect of the asymmetry of a structure is compensated by an extension of the beam's flange.

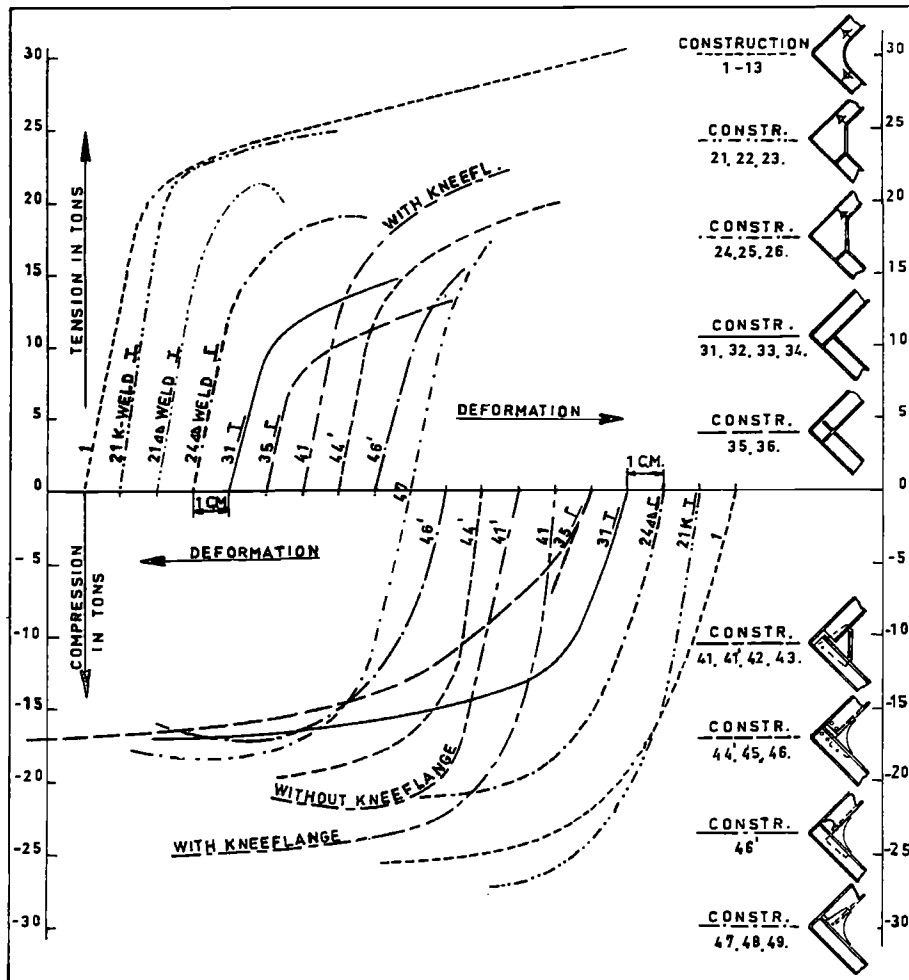


Fig. 30

2. The maximum bending moment supported is at least 70 % of that of the moment supported by the ideal knee of same dimensions.
3. An inconvenience of the connections orthogonally butt welded without knees is the lack of rigidity.
4. The elastic limit of the bracketed connections 31 and 35 is only 58 % and 49 % respectively of the elastic limit of the ideal knee-connection.
5. The resistance to compression of types 44 and 47 is only 75 % of that of the ideal knee. This resistance is only 66 % of that of the ideal knee with test-piece No. 46', which is even lower than that of types 31 to 36. In appendix III data about the knees described in [12] with overlaps of other dimensions are given and scale-effects are considered.
6. The reserve against plastic compression remains high with all the test-pieces. The proportion $\frac{M_{\text{maximum}}}{M_{\text{elastic limit}}}$ is more than 1.5 for ideal knees and asymmetric triangular knees. For the other types of test-pieces this proportion reaches 2.

It must be kept in mind that with the ideal knees the failure load under tension was never at-

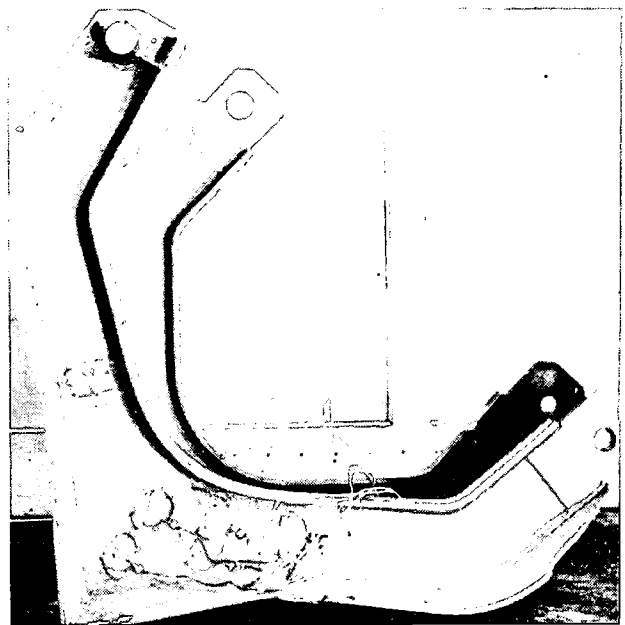


Fig. 31. Ideal structure after tensile test

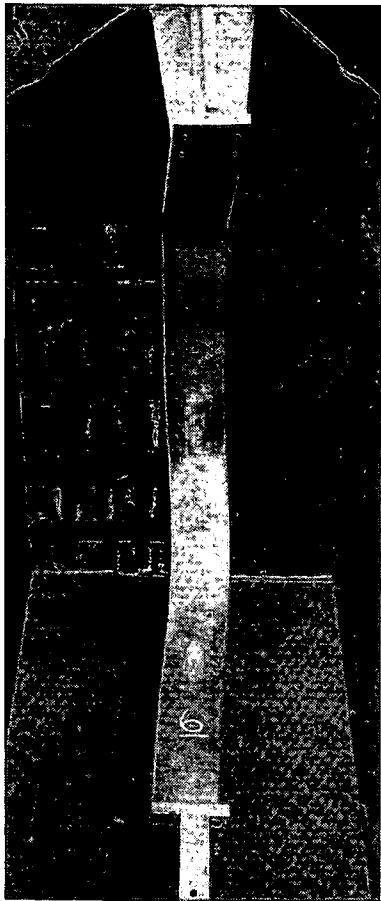


Fig. 32. *Ideal structure after compressive test*

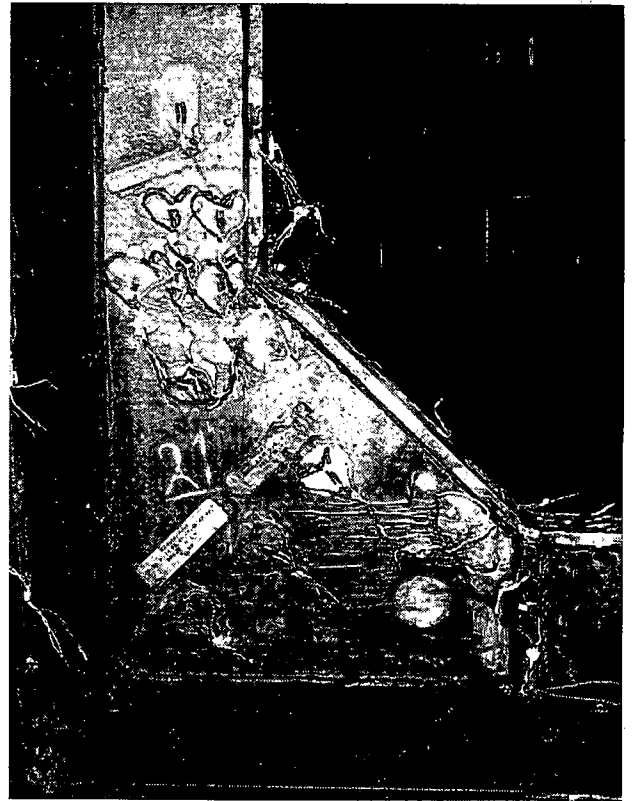


Fig. 33. *Triangular bracket after compressive test (T-section)*

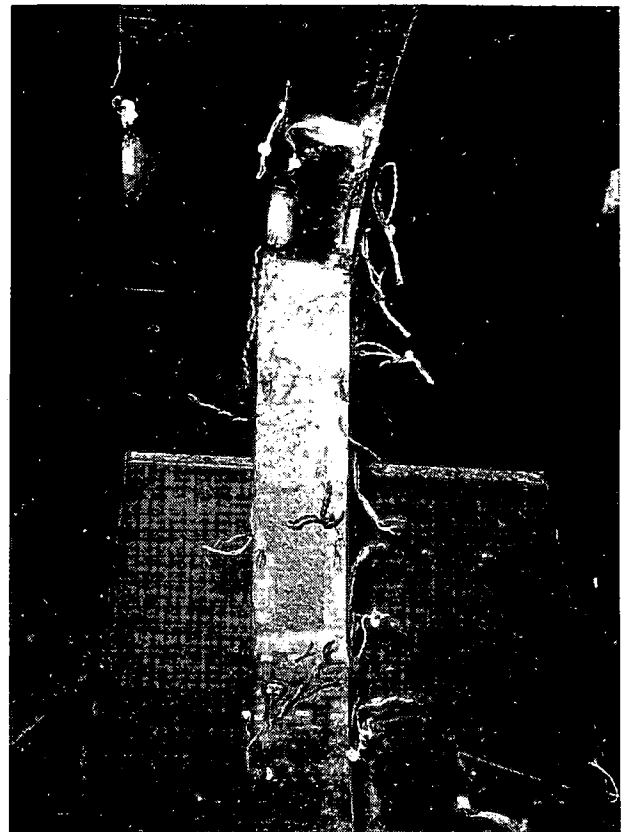
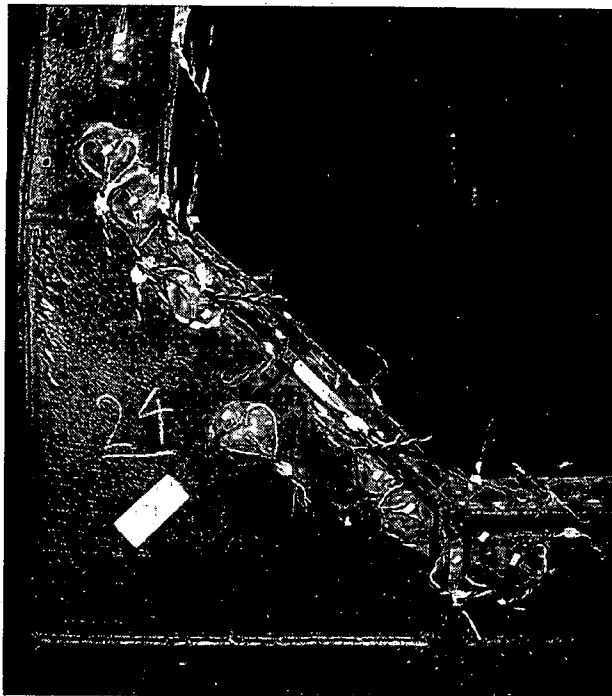


Fig. 34. *Triangular bracket after compressive test: L-section*

tained. Indeed the plastic deformations were greater than the free way of the testing machinery and no definite values for this plastic deformation could be measured (see fig. 31).

The triangular knees are under traction certainly stronger with K-welded knees than with fillet-welds. Figures 32 to 41 give an impression of the conditions of different test-pieces after the static tests. With the triangular knees and the orthogonally butt welded beams and frames, the favorable influence of tripping brackets and prolongation of flanges relative to compression loads is manifest.

§7. Checking calculations

For checking purposes a method of calculation was developed, as described in appendix II.

This method is based on the assumption that the test-pieces are heavily curved beams with a variable

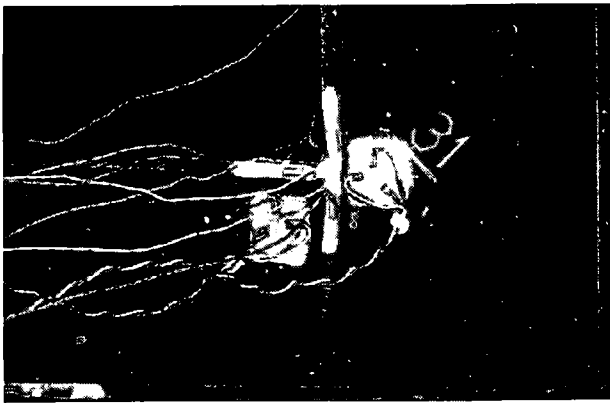


Fig. 35. Bracketless construction after compressive test (T-section)



Fig. 36. Bracketless construction after compressive test: L-section

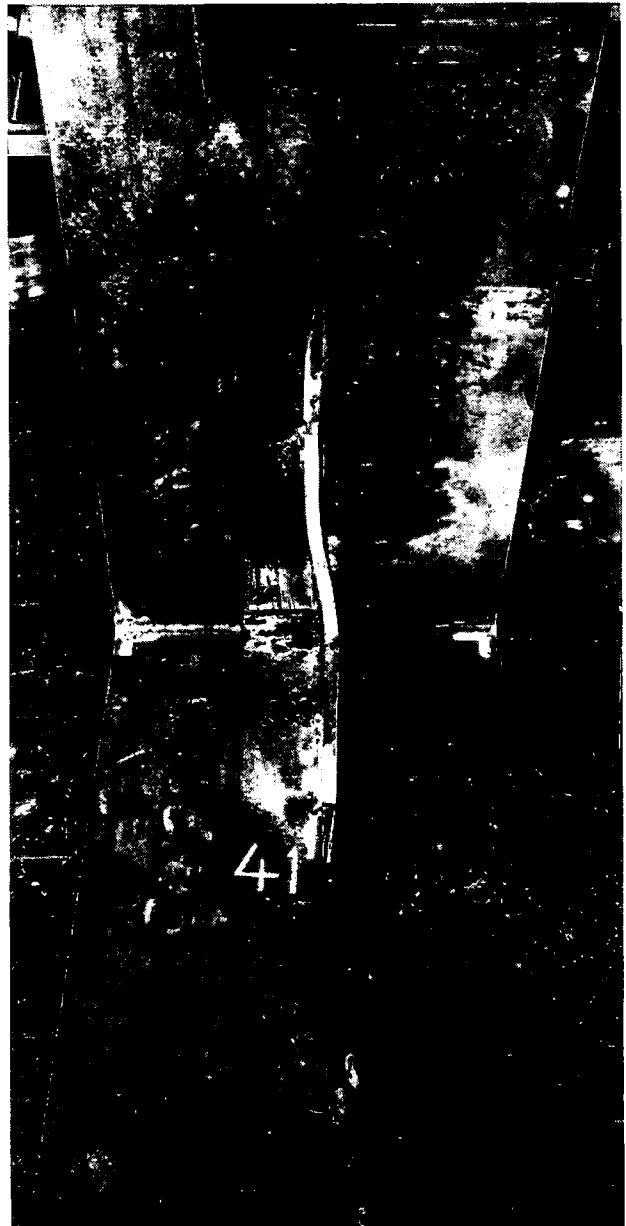


Fig. 37. Construction no. 41' after compressive test

height and a variable flange-efficiency. The latter is determined by the method shown in figure 9 by means of measurements.

The orthogonal joint of adjacent structural members at the corner of deck- and hull-plates has as a consequence that the stresses in that corner become negligible. The loads in the hull and the deck are transmitted to the coaming of the knee by shearing forces and the normal stresses in the hull and the deck therefore become less.

Due to secondary bending (fig. 19) the values of the stresses in the curved flanges are not directly proportional to the strains $E \varepsilon$ (see § 5). This is clear, when observing section F, where the stress calculated *) is 17 % higher than the one measured,

*) According to bending theory.

but only 3 % higher than the measured strain E_s .

The values of E_s measured and calculated are in good concordance along the flange (see fig. 13 for the ideal knee No. 9, and fig. 14 for the ideal knee No. 13). It is therefore clear that, though section F can be calculated on the straight-beam theory, at 15° further it is necessary to apply the formulae of the curved beam theory.

In figures 13 and 14 there are also given curves representing stresses at half-thickness calculated by the *Vierendeel*-method (see appendix II). Though objections are indicated in this appendix, the con-



Fig. 38. Construction no. 42 after compressive test



Fig. 39. Construction no. 44 after compressive test

cordance between calculation and measurements is satisfactory. This simple method can be used therefore, when a rapid verification is sufficient.

The stresses in the flanges of triangular knees also may be calculated approximatively by the *Vierendeel*-method. In this case the stresses calculated at the inner flanges at some distance from the breaks are always higher than the real ones (maximum difference observed = about 30 %). Thus for types 41, 41' and 47 the *Vierendeel*-method is a sufficient and safe approximation.

For the orthogonally butt welded beam-frame construction without brackets *Osgood* [7] has developed a calculation-method. However, in this case, as well as in the foregoing ones, the stress-concentrations cannot be calculated.

Table II gives the data obtained during the tests. It must be kept in mind that at points of stress-

concentration the values determined by these tests are influenced by the positions and the dimensions of the test-pieces (see the end of appendix III).

§8. The dynamic tests

The stress-concentrations as described in §5 are very important when dynamic loads are applied. Tables I and II and figure 42 indicate the results of the dynamic tests of all test-pieces. The dynamic load was applied by means of an *Amsler* pulsator [14].

On a primary static load S a variable load $2P$ was superimposed (see fig. 42). For nearly all the tests P was kept constant, while a different value for S was chosen for all test-pieces. This was the only practical way to introduce these loads with the *Amsler* machinery and at the same time it was thought that this was a realistic way to deal with this problem. Thus S represented the loading conditions of the ship, while P represented the outside loads expected due to the seaway.

The idea was to reproduce the phenomenon of high stress low cycle fatigue as described in [2] and

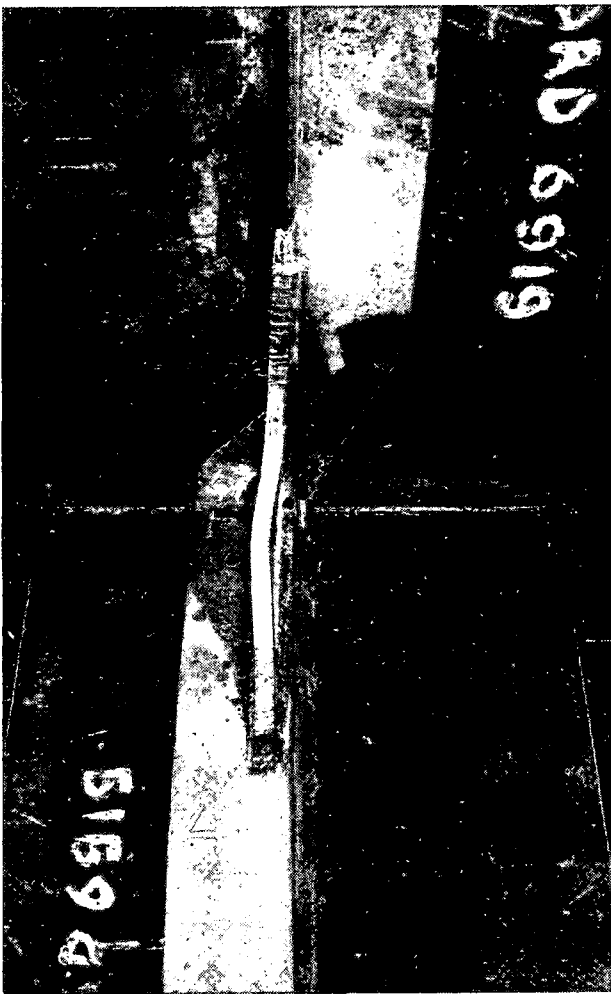


Fig. 40. Construction no. 47 after compressive test

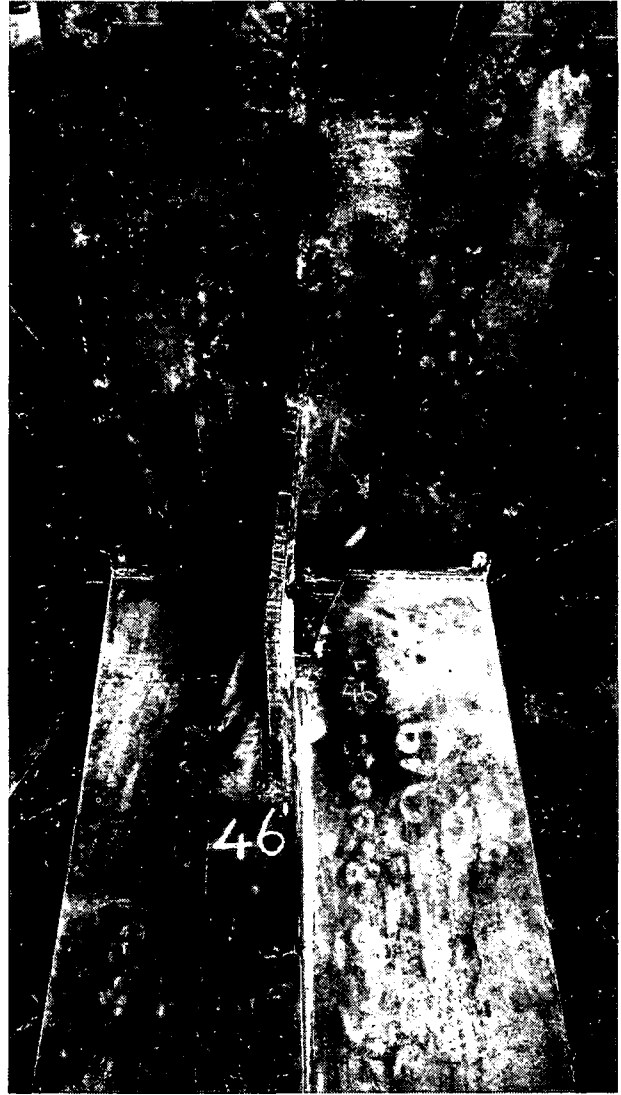


Fig. 41. Construction no. 46' after compressive test

[3], due to an accumulation of strains. As the ideal knee was designed so as not to have stress-concentrations, this type of test-piece did not show the phenomenon at the loads applied by the *Amsler* pulsator.

The variable load P was fixed by the maximum amplitude of the pulsator, which was 6,3 mm. The corresponding value of $2P$ was generally 7,8 tons.

The results of the dynamic tests are given in figure 42, as already stated for all types of test-pieces. The values indicated by the smallest symbols (see table II) are the directly measured ones (see table I). The symbols in medium size type indicate the mean results for each type of test-piece, while the symbols in large type give the corrected results in order to obtain a good comparison between the different types of knees. This is done in the following way:

The mean results are transformed into mean moments. The arm of the applied loads to the ideal knees and the triangular knees is supposed to be

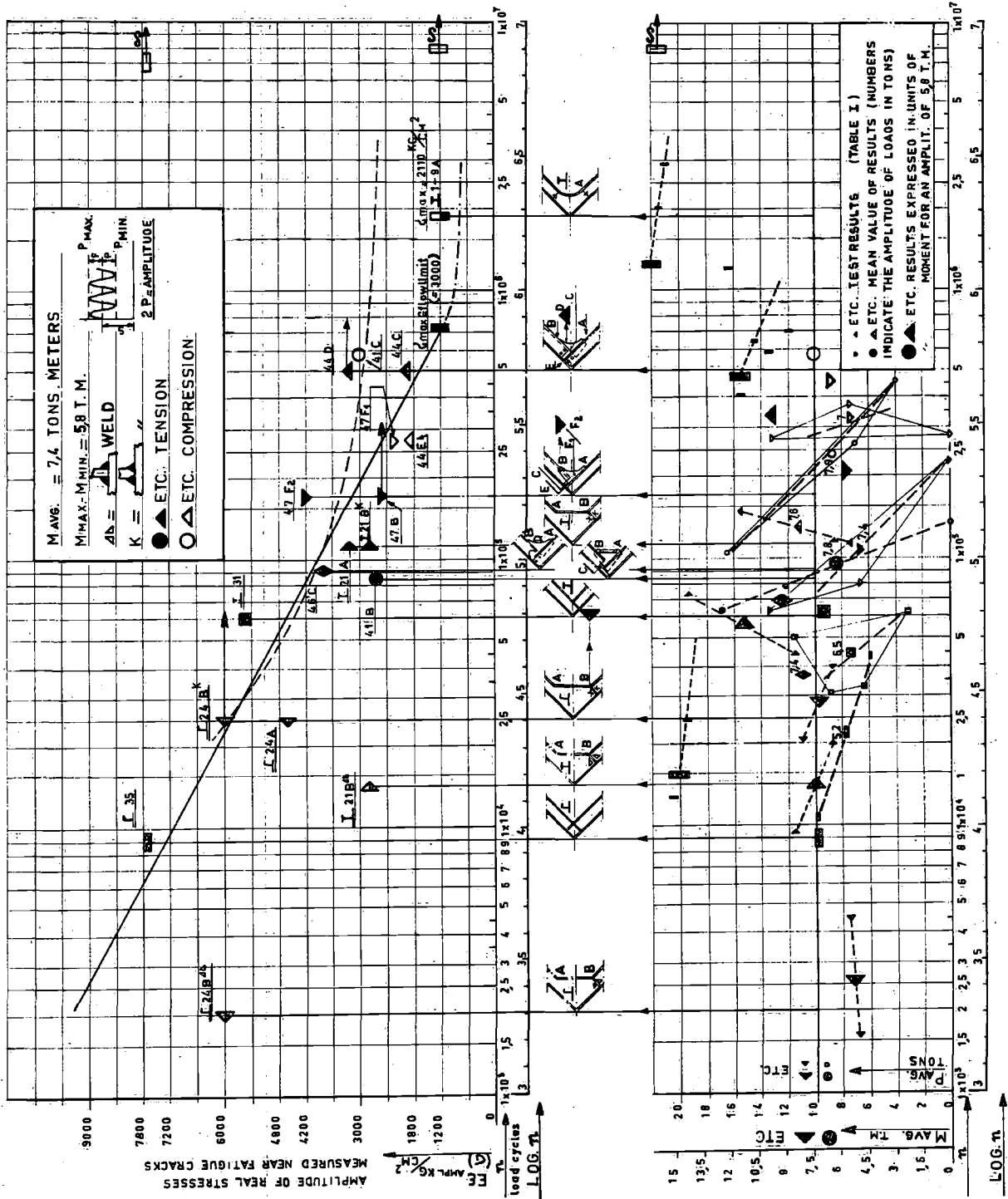


Fig: 42

quasi-constant viz. 0,74 m. The lower diagram of figure 42 is so drawn, that 0,74 m.ton corresponds to the scale of 1 ton. Then the symbols in large type all refer to an amplitude of moment of

$7,8 \text{ ton} \times 0,74 \text{ m} = 5,8 \text{ m.ton}$, base to which all results are reduced. As the average moment for most of these large symbols is about 7,4 m.ton, the $M_{avg} = 7,4 \text{ m.ton}$ conforms to the scale of 10 ton load.

The scale of the dynamic load which a construction can support, is given as the logarithm of the number of cycles. The dotted lines in figure 42 (lower diagram) represent the direct measured results. By means of these lines the representative values for the various test-pieces for $M_{avg} = 7,4 \text{ m.ton}$ are constructed (table II). The photographs Nos. 43 to 58 give an impression of the condition of different test-pieces after the dynamic tests. The places where fatigue-cracks were formed, are indicated by letters in large type corresponding to tables I and II.

§ 9. Conclusions and general considerations derived from the test-results

In table II all results are analysed in giving them a constructive scale-value varying from 1 to 5.

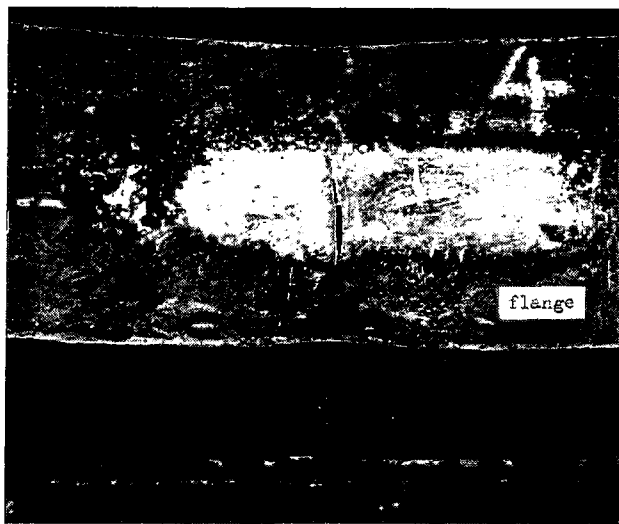


Fig. 43. Flange of ideal structure no. 4 after dynamic test (tension)

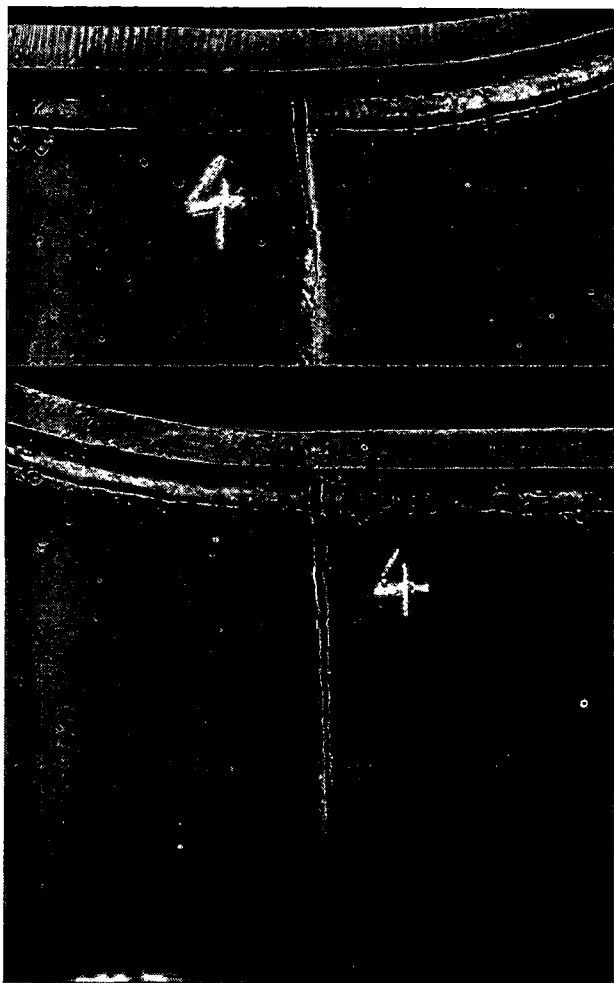


Fig. 44. Face and reverse side of web of ideal structure no. 4

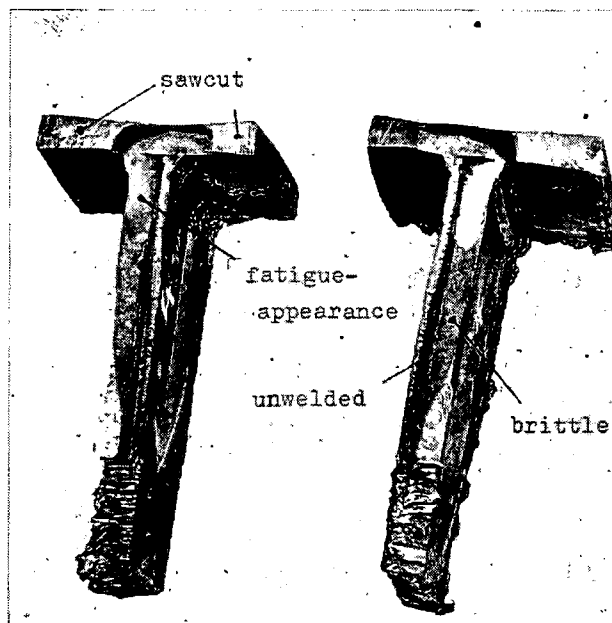


Fig. 45. End view of fracture shown in figures 43 and 44

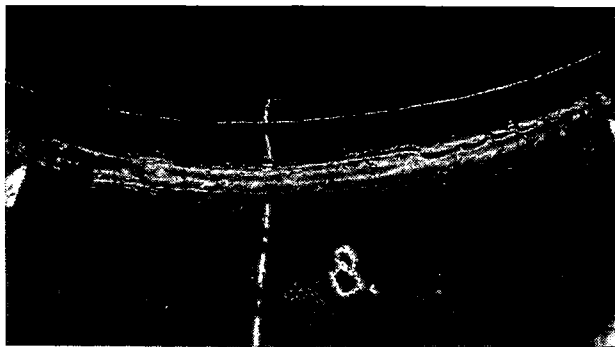


Fig. 46. Fracture between flange and web of ideal structure no. 8 (dynamic tension)

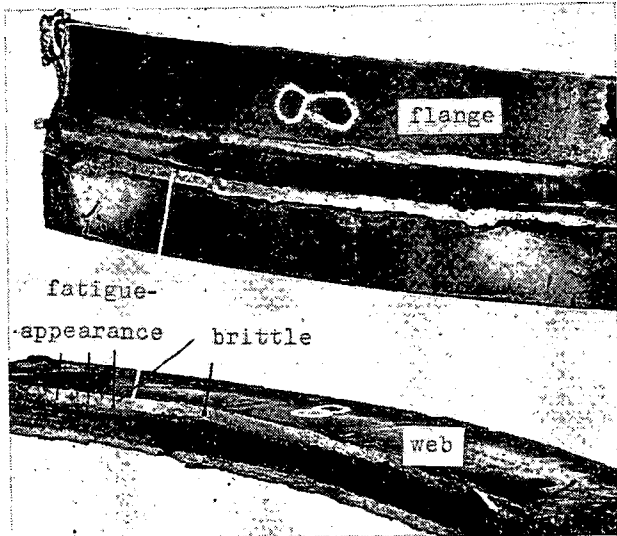


Fig. 47. End view of fracture shown in fig. 46



Fig. 50. Crack in beam at point B of no. 42 (dynamic tension)

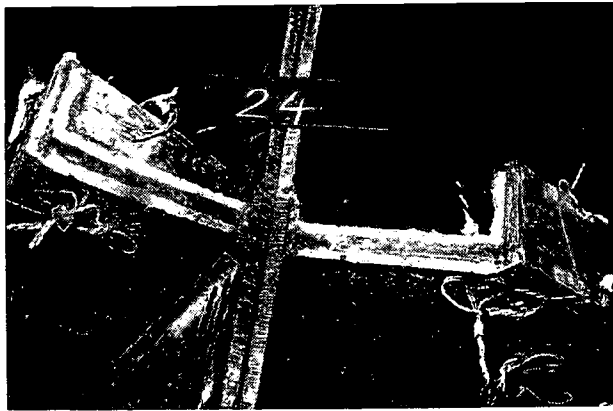


Fig. 48. End view of fracture in filletwelded structure 24

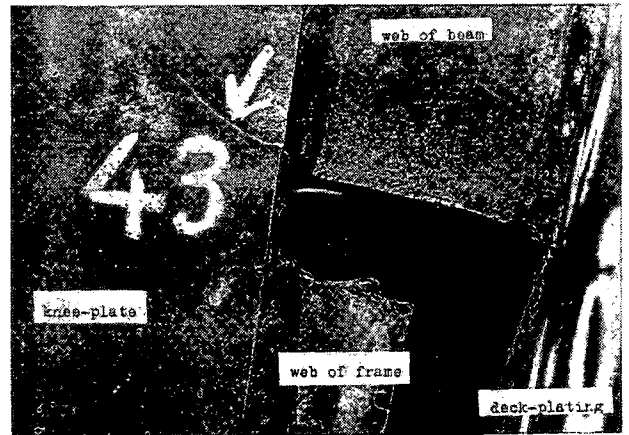


Fig. 51. Crack in kneeplate at point C of no. 43 (dynamic compression)

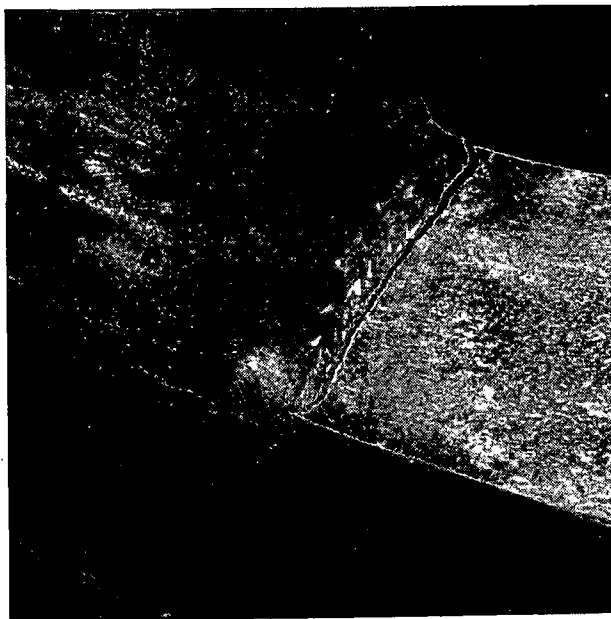


Fig. 49. Crack in bracketless construction no. 34 (dynamic tension)

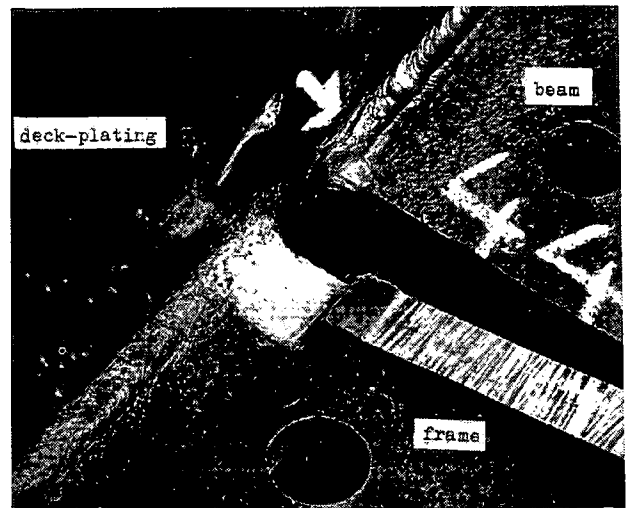


Fig. 52. Crack in end-weld, connecting beam to deck-plating (dynamic tension; point E' of no. 44)

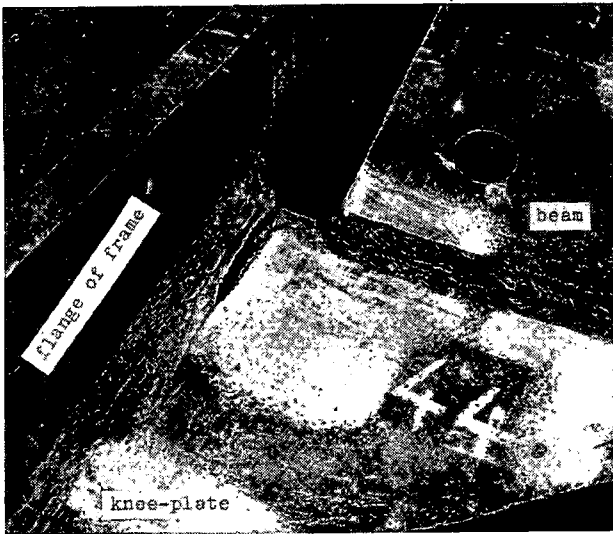


Fig. 53. Crack in kneeplate near frame (dynamic tension, point C of no. 44)

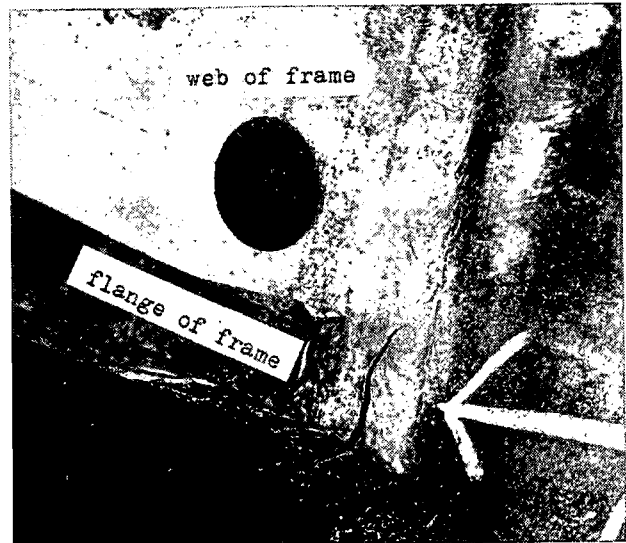


Fig. 54. Tiny crack in end-weld connecting frame to deck (dynamic compression; point E of no. 46)

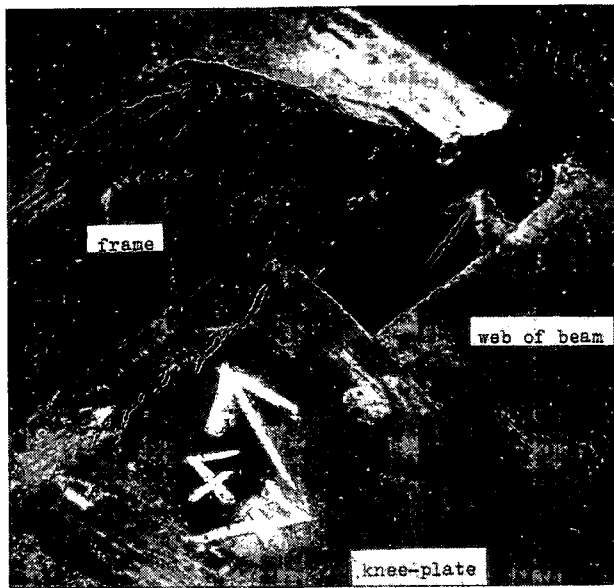


Fig. 55. Cracks in kneeplate of no. 47 (dynamic compression F_1)

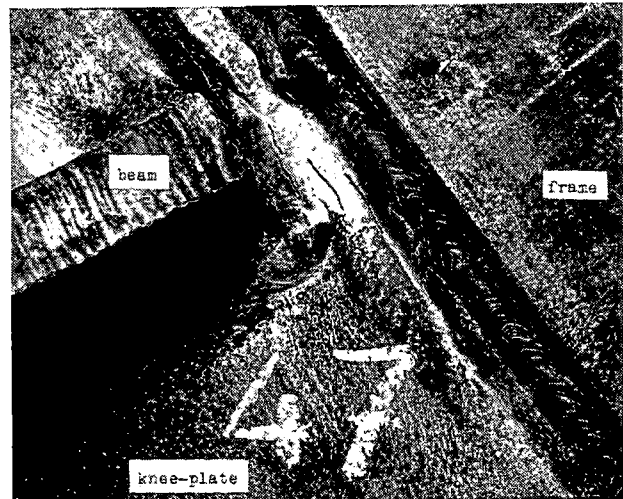


Fig. 57. Tiny cracks in kneeplate at end of beam (dynamic tension point F_2 of no. 47)

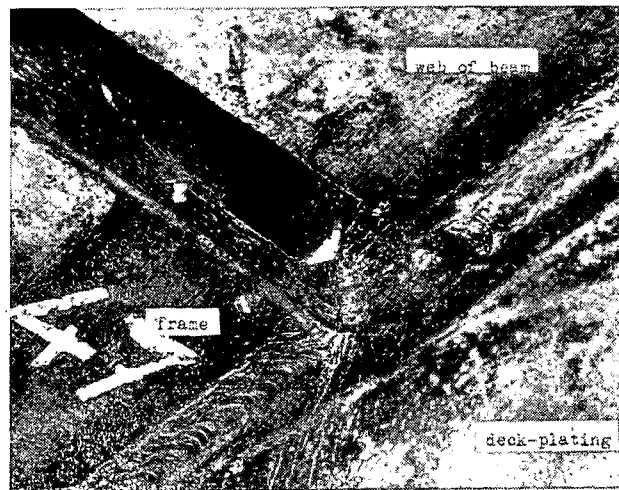


Fig. 56. Tiny crack in end-weld, connecting frame to deckplating (dynamic compression; point E of no. 47)

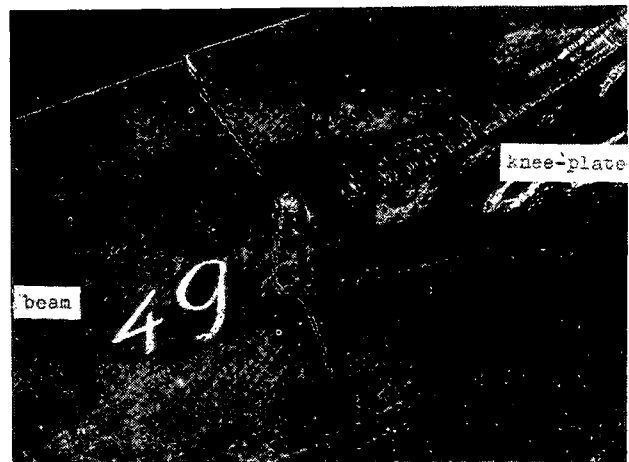


Fig. 58. Crack in beam at point B of no. 49 (dynamic tension)

TABLE II

1	2	3	4		5		6		7		8		9		10-13			
			ELASTIC STRESSES				RELATION BETWEEN LOG n OF IDEAL KNEE AND LOG n OF OTHER CONSTRUCTIONS. THE IDEAL STRUCTURE IS INDICATED BY 1				MOMENT OF LOAD		QUALIFICATION OF CONSTRUCTION					
			RELATION BETWEEN STRESSES IN ALL TYPES OF KNEES AND IN IDEAL STRUCTURE FOR EQUAL MOMENTS	RELATION BETWEEN STRESSES IN ALL TYPES OF KNEES AND IN IDEAL STRUCTURE FOR EQUAL FORCES	TENSION	COMPRESSION	TENSION AND COMPR. AT FLOW LIMIT	COMPRESSION AT COLLAPS	STATIC TENSION AND COMPR AT FLOW LIMIT	STATIC COMPRESSION AT COLLAPS	DYNAMIC TENSION	DYNAMIC COMPRESSION						
	1.9A	1.2	1	1	1	>> 1	1	1	1	1	1	1	1	1	1	1	1	1
	21A	2.85	2.74	2.74	0.81	>> 1	0.61	0.92	3	1	2	1						
	21B ^{ab}	2.4	2.32	2.32	0.66	>> 1				1	4	1						
	21B ^k	2.4	2.32	2.32	0.81	>> 1				2	1							
	24A	2.2	3.92	3.92	0.70	>> 1	0.70		3	3	3	1						
	24B ^{ab}	2.8	5.08	5.08	0.54	>> 1			3	2	5	1						
	24B ^k	2.8	5.08	5.08	0.77					3	1							
	31	4.2	4.75	6.08	0.76	>> 1	0.58	0.71	4	3	3	1						
	35	3.4	6.86	8.78	0.63	>> 1	0.49	0.71	4	3	4	1						
	41A	1.3	2.20	2.20	0.80	>> 1			4	2	3	2						
	" B	1.3	2.20	2.20	0.79	>> 1	0.56	0.83										
	" B		2.75	2.75														
	" C		2.54	2.88		0.92												
	41ssA	1.2	1.28	1.28			0.56		4	2	3	2						
	" C		1.01	1.16				0.85										
	44A	1.2	2.09	2.09	0.98	>> 1			4									
	" B	1.2			> 1	>> 1												
	" C		1.70	1.70	0.91	> 1	0.56		4	2	2	3						
	" D		2.71	3.10	0.94	>> 1		0.77										
	" E		1.58	1.83	>> 1	0.87												
	46A	1.0	2.09	2.09			0.31		5	4	3	3						
	" C		3.39	3.95	0.79			0.66										
	" D		2.58	3.10														
	47A	1.2			> 1	>> 1			4									
	" B	1.2	2.12	2.12	0.88	>> 1												
	" C1		1.74	2.03	> 1	0.96												
	" D		1.85	2.16			0.56		4	3	2	3						
	" F1		1.95	2.26	>> 1	0.88												
	" C2		1.33	1.56	0.98	>> 1												
	" F2		3.56	4.18	0.83	>> 1		0.73										

OBSERVATIONS: a) IN COLUMNS 4,5,6,7,8,9 THE RELATIONS BETWEEN VALUES OF ALL TYPES OF KNEES AND THE IDEAL STRUCTURE ARE GIVEN. FRAMED VALUES IN COLUMNS 6 AND 7 ARE MEASURED; SMALL FIGURES INDICATE ESTIMATIONS >> 1 LOG n > 7, > 1 LOG n = 6.5 TO 7 b) IN COLUMNS 10,11,12,13 FIGURES OF QUALIFICATIONS ARE GIVEN VARYING FROM 1 TO 5 1 INDICATING THE BEST STRUCTURE.

This scale may help the naval architect, whenever there is a connection-problem to solve where the loading conditions are known. The other columns in the table give complementary information about the strength properties of the chosen type of connection.

In § 1 it is explained why dynamic tests must be made to obtain an exact opinion about the structural value of a construction. On the other hand static tests are important to obtain a good idea about the magnitude of stress-concentrations and collapse-loads.

Dynamic tests with full-scale constructions are very expensive.

Therefore it is highly desirable to obtain information from static tests which can act as a criterion for dynamic strength.

There is no doubt that none of the four aspects of static strength (as mentioned at the end of § 1) will serve our purpose.

It seems that the magnitude of stress-concentrations is a good criterion for judging a dynamically loaded structure, especially if these loads are traction-loads. In our tests we have the particular case of structures dynamically bent in such a way, that the maximum value of the bending moment is large enough to bring the structure into the plastic condition.

The loads were not sufficiently high for the fully plastic condition to be reached in any section of the structure.

In consequence the deformation in the extreme layers of the sections of the test-pieces were restricted to values where little or no strain hardening of the material could occur.

As a result of this the maximum value of the stresses could not exceed the flow limit. The initiation of cracks in the test-pieces then must mainly be governed by the dynamic part of the load viz. the magnitude of the amplitude.

As previously stated, all our test-results were reduced to the dynamic strength for each type at a load with an amplitude of 5,8 tm and a mean value of 7,4 tm*). Accordingly differences in time of initiation of cracks in the various types of structures can only be due to differences in the magnitude of the stresses in these places.

In the upper part of figure 42 the local stresses ($\sigma_{amplitude}$ see fig. 42) at parts where cracks developed, are given at a load of 5,8 tm as a function of the number of cycles for the above mentioned load condition.

A few horizontal arrows in figure 42 indicate the supposed dynamic resistance of some structural details where small fatigue-cracks had been observed; in reality these test-pieces failed in other places. After all a mean „fatigue-line” could be

traced, and this became a straight line, which has as equation:

$$\log n = 6,20 - 0,314 \cdot 10^{-3} \cdot \sigma_{amplitude}^{**})$$

This “fatigue-line” is compared to the one given for steel 42, normal ship’s steel (dotted line), for so far such a line for steel 42 could be determined as a result of the publications of different laboratories. Though there are up to the present not many ideas about this question, there seems to be a certain analogy between both lines till the frequency of $n < 10^5$. This will be due to the fact that the time for the development from a small crack to a complete fracture is nearly independent of the original stress concentration that is caused by weld defects and similar stress-raisers. In these frequency-regions this time of development is long in proportion to the total time till failure. All cracks, whether due to stress-concentration or not, begin at places where tensions are high.

High dynamic compression stresses are not dangerous. Therefore all types, except the “overlap” types, have a great resistance to important dynamic compressions (see test-pieces 11 and 36). The overlap types in fact show large tensile stresses when the external load is compressive.

When tracing the “fatigue-line”, the test-pieces 22B, 23B, 25B and 26B were not taken into consideration. In these cases shrinkage-cracks were already present when the dynamic tests started. The great differences between the “fatigue-line” and the black symbols for the types 41B and 44D are explained by the very special positions of the measuring strain-gauges in these cases (see end of appendix III).

Knees are very numerous on board ship. Some are statically loaded, others dynamically. Quite a number undergo high stresses or stress-concentrations. In practice it is not always easy to realise exactly how the knee is loaded. As already said in § 1, the knee-construction is still often based on erroneous ideas about “fixed-end” connections and old-fashioned “riveted” designs.

Quite another point is the assumption of the rigidity of the bracketed connection, and in all the calculations of § 7 it was assumed that the joints were rigid in that all the structural members meeting at such a joint turned through the same angle when the structure was loaded. The tests performed afforded an opportunity to prove the validity of this generally adopted assumption and to obtain some indication of the rigidity provided by different welded bracketed connections.

It became clear also that the best constructed brackets do not necessarily use their full “fixed-end” effect, as the moment caused by the load works at another place. Moreover, knees are often

*) At this load only the stresses in the ideal kneetype did not reach the flow limit, so that a correction was necessary.

***) If the values of $\sigma_{amplitude}$ are high, it is more realistic to use $E\epsilon_{amplitude}$.

too heavily constructed, if the constructor does not consider what kind of loads the bracket-connection must carry. He then may diminish the scantlings of the construction or even do away altogether with the knee in butt-welding the orthogonally placed adjacent members, such as beams and frames.

The ideal knees are the best from every point of view except that they are more expensive. The static and dynamic properties are better adapted to the sections (beams and frames). Moreover, with dynamically loaded bracketed connections a good weld in the tension-part is absolutely vital. Only first class quality welds of full penetration are acceptable and therefore it is necessary to avoid as much as possible welding in difficult positions.

That fillet-welds are much worse than K-welds in dynamically loaded structures, has been known for years. These tests again proved their unsuitability in this respect.

The following main conclusions may be drawn:

1. It is as important to have good welding as to have good welding-construction-design. A bad weld destroys all the good influences a good design may introduce.
2. Constructions symmetric to the bracket-plane are preferable.
3. When important static compression loads are present, tripping brackets are absolutely necessary with asymmetric knees and preferable with symmetric ones.
4. Rounded knees are preferable especially when loads are dynamic. These knees must be butt welded. Ideal knees are the best form of bracketed connections.
5. In principle a corner constructed with symmetric sections, is as good without brackets as an asymmetric structure with overlapping brackets or triangular knees. The resistance against compression remains about 70% of that with ideal knees, a value not exceeded by the overlap-knees and triangular knees. This resistance may be even more, when tripping brackets are fitted judiciously in the sections.
6. Overlapping knee-plates must be condemned, as they introduce secondary deflections.
7. A spare hole in the end of a section (beam or frame) is always bad.
8. The resistance of a bracketed connection to dynamical compression is always better than it is to dynamic traction.
9. Fatigue-cracks only originate when high traction stresses are present and are often combined with welding-cracks (stress-concentrations).
10. A correlation is found between the number of cycles to fatigue-failure and the magnitude of the strains at the point of failure.

11. Stress-concentrations are more dangerous with average dynamic loads and a high number of cycles ($n > 10^5$) than with high dynamic loads and a low number of cycles ($n < 10^5$) (see fig. 42).

§ 10. Acknowledgements

The authors express their appreciation for the valuable help which they received from the "Rotterdamse Droogdok Maatschappij" at Rotterdam, who fabricated all test-pieces, for the financial help of the Netherlands Shipbuilding Research Association and for the direct help received from the staff of the Ship Structure Laboratory of the Technological University at Delft and specially by the draughtsman Mr. J. van Lint. They also thank the "Instituut voor Werktuigbouwkundige Constructies T.N.O. "I.W.E.C.O." for the use of their self-designed, self-registrating measurement apparatus of 48 measuring points each.

Bibliography

1. Opie, B. P.: "An investigation into the behaviour and influence of welded bracketed connections in aluminium alloy structural members". Trans. Institution of Naval Architects, Vol. 99, London, 1957.
2. Jaeger, H. E.: "Observations sur les essais dynamiques d'éprouvettes à hautes contraintes ou à concentration de contraintes". Bulletin de l'Association Technique Maritime et Aéronautique No. 57, Mémoire 1230, pages 645-661, Paris, 1958.
3. Nibbering, J. J. W.: "Enige beschouwingen over breukverschijnselen, sterktecriteria en constructieve vormgeving, in het bijzonder met betrekking tot scheepsconstructies". Schip en Werf, Rotterdam, 12 June 1959.
4. Garmo, E. P. de: "Tests of various designs of welded hatch-corners for ships". The Welding Journal, New York, February 1948.
5. Irwin, L. K. and Campbell, W. R.: "Tensile tests of large specimens representing the intersection of a bottom longitudinal with a transverse bulkhead in welded tankers". Final Report SSC-68 of the Ship Structure Committee, Washington D.C., 18 January 1954.
6. Jaeger, H. E.: "Il problema della concentrazione delle sollecitazioni a bordo delle navi". Tecnica Italiana, Anno XXIII, no. 1 and no. 2, Trieste, January-April 1958.
7. Stang, A. H., Osgood, W. R. and Greenspan, M.: "Strength of a riveted steel rigid frame having straight flanges". Journal of Research of the National Bureau of Standards, Volume 21, page 853, Washington D.C., 1938.
8. Stang, A. H. and Greenspan, M.: "Strength of a riveted steel rigid frame having curved flanges". Journal of Research of the National Bureau of Standards, Vol. 27, page 443. Washington D.C., 1938.
9. Topractsoglou, A. A., Beedle, L. S. and Johnston, J. N.: "Connections for welded continuous portal frames". Welding Research Council, Vol. 19, pages 359 and 397 and Welding Research Council, Vol. 17, page 543, New York, 1951-1952.
10. Wright, D. T.: "The design of knee-joints for rigid steel frames". British Welding Journal, Vol. 4, No. 6, London, June 1957.
11. Kerkhof, W. P.: "Beschouwingen over de vormgeving van gelaste scheepsconstructies". Symposium, pages 5-22, Utrecht, 1951.
12. Gätz, J. R., Lovstad, C. D. and Moen, K.: "Kneplatter". Skip-teknisk Forsknings Institutt, No. 8, Oslo, 1955.
13. Haigh, B. P.: "Constructional tests on mild steel rolled sections with electrically welded joints". Trans. Institution of Naval Architects, Vol. 75, pages 59-68, London, 1933.

14. Jaeger, H. E. and Does, J. C. de: "A modern laboratory for tests and research on ships structures". International Shipbuilding Progress, Vol. 4, No. 30, Rotterdam, February 1957.
15. Hendry, A. W.: "An investigation of the stress distribution in steel portal frame knees". Structural Engineering, Vol. 25, pages 101-141, London, 1947.
16. Grashof, F.: "Elastizität und Festigkeit", Berlin, 1878.
17. Jaeger, H. E. and Nibbering, J. J. W.: "La résistance des connexions à goussets". Bulletin de l'Association Technique Maritime et Aéronautique, No. 59, Mémoire No. 1257, pages 273-316, Paris, 1959.
18. Jaeger, H. E. and Nibbering, J. J. W.: "La résistance des connexions à goussets II". Bulletin de l'Association Technique Maritime et Aéronautique". No. 60, Mémoire No. 1282, pages 151-171, Paris, 1960.

APPENDIX I

TENSILE TESTS MADE FOR THE MATERIAL USED

A. Material for ideal knees

	For annealed and non-annealed tensile test-pieces	
	13 mm	16 mm
Thickness	13 mm	16 mm
Flow limit	2700 kg/cm ²	3215 kg/cm ²
σ_B (failure)	4515 kg/cm ²	4435 kg/cm ²
Elongation at failure	27.5 %	28.1 %

B. Material for triangular knees

a) Material for the hull and the deck-plates, thickness 13 mm

	Annealed	Non-annealed
Flow limit	2750 kg/cm ²	2905 kg/cm ²
σ_B (failure)	4235 kg/cm ²	4325 kg/cm ²
Elongation at failure	29.4 %	29.4 %

b) Material for the flange and coaming-plates for symmetric knees, thickness 16 mm

	Annealed	Non-annealed
Flow limit	2690 kg/cm ²	3060 kg/cm ²
σ_B (failure)	4120 kg/cm ²	4180 kg/cm ²
Elongation at failure	30.0 %	31.1 %

c) Material for the sections of the asymmetric knees, thickness 16 mm

	Annealed	Non-annealed
Flow limit	2320 kg/cm ²	2450 kg/cm ²
σ_B (failure)	4230 kg/cm ²	4210 kg/cm ²
Elongation at failure	29.7 %	28.7 %

d) Material for the bracket of the asymmetric knees, plate-thickness 16 mm

	Annealed	Non-annealed
Flow limit	2760 kg/cm ²	
σ_B (failure)	4125 kg/cm ²	
Elongation at failure	31.6 %	

C. Material for real knees

a) Material for the hull and the deck-plates, thickness 13 mm

	Annealed	Non-annealed
Flow limit	2830 kg/cm ²	3040 kg/cm ²
σ_B (failure)	4300 kg/cm ²	4440 kg/cm ²
Elongation at failure	28.5 %	26.0 %

b) Material for the sections, thickness 16 mm

	Annealed	Non-annealed
Flow limit	3120 kg/cm ²	3040 kg/cm ²
σ_B (failure)	4400 kg/cm ²	4500 kg/cm ²
Elongation at failure	25.0 %	25.0 %

c) Material for the bracket; plate thickness 16 mm

	Annealed	Non-annealed
Flow limit	2520 kg/cm ²	2580 kg/cm ²
σ_B (failure)	4400 kg/cm ²	4640 kg/cm ²
Elongation at failure	25.0 %	29.0 %

APPENDIX II

CALCULATIONS FOR IDEAL KNEES

a) Vierendeel-method [15] (see fig. 59)

The stresses at the section x - x at the half-thickness of the plates (flanges, hull and deck) are

$$f_i = \frac{H}{A} - \frac{M}{J} a_i$$

$$f_o = \frac{H}{A} + \frac{M}{J} a_o$$

$$A = b \cdot d + F_o + F_i \cos \alpha$$

$$J = \frac{b \cdot d^3}{12} + F_o a_o^2 + F_i \cos \alpha \cdot a_i^2$$

where

a_o and a_i = distances between the centres of gravity of the plates and the centre of gravity of the total section;

F_o and F_i = section of the hull and the flange;

b and d = thickness and height of the coaming at section x - x.

In this way the method in fact determines the stresses of a part S of a structure indicated in figure 60 (which is not an orthogonally bracketed connection). In figures 12 and 13 the calculated stresses by the Vierendeel-method are indicated for test-pieces 9 and 13. The result of the calculation is in good accordance with the measurements. For the hull and the deck the calculation for the ex-

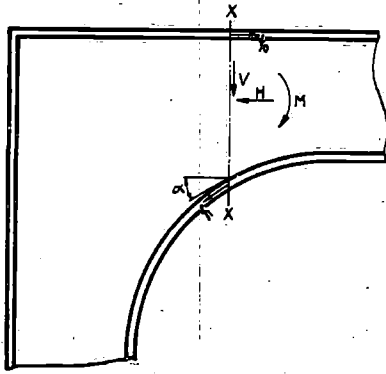


Fig. 59

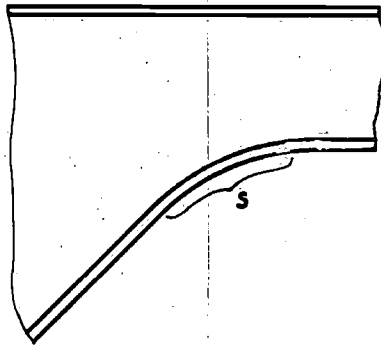


Fig. 60

terior of the plates corresponds well within the limited zone indicated by *Vierendeel*.

b) *Curved-beam-method*

The ideal knee is here considered as a curved beam of special form. *Grashof* [16] admits that plane sections of a curved beam remain plane after loading (see fig 61).

The neutral axis NA_x is not the same as the centre-line $Z - Z$. The elongation of this centre-line becomes:

$$\epsilon_0 = \frac{zz'}{R_z \cdot d\varphi}$$

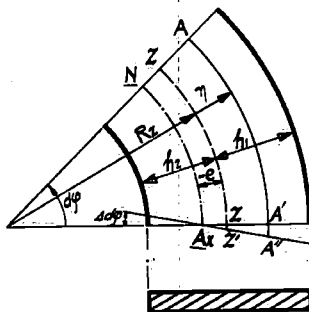


Fig. 61

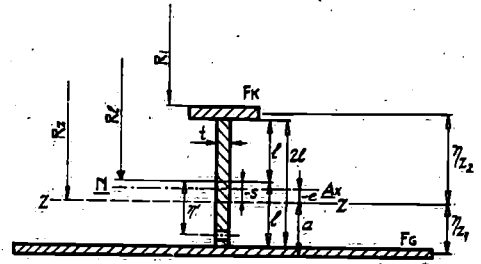


Fig. 62

The elongation of a layer at the distance η from the centre-line becomes:

$$\epsilon\eta = \frac{AA'' - AA'}{AA'} = \frac{zz' + \eta \Delta d\varphi}{(R_z + \eta) d\varphi} = \frac{\epsilon_0 R_z d\varphi + \eta \Delta d\varphi}{(R_z + \eta) d\varphi}$$

or, as

$$\omega = \frac{\Delta d\varphi}{d\varphi}$$

we find:

$$\epsilon\eta = \epsilon_0 + \frac{\eta (\omega - \epsilon_0)}{R_z + \eta} \dots \dots \dots (1)$$

$$\sigma_\eta = E\epsilon_\eta \dots \dots \dots (2)$$

$$N = \int_{-h_2}^{h_1} \sigma_\eta \cdot dF = E\epsilon_0 F + E \int_{-h_2}^{h_1} (\omega - \epsilon_0) \frac{\eta}{R_z + \eta} \cdot dF \dots \dots \dots (3)$$

$$M_z = \int_{-h_2}^{h_1} \sigma_\eta \cdot \eta \cdot dF =$$

$$E \int_{-h_2}^{h_1} \left\{ \epsilon_0 + \frac{\eta (\omega - \epsilon_0)}{R_z + \eta} \right\} \eta \cdot dF =$$

$$= E \int_{-h_2}^{h_1} \left\{ \frac{R_z \cdot \epsilon_0 \cdot \eta \cdot dF}{R_z + \eta} + \frac{\omega \cdot \eta^2 \cdot dF}{R_z + \eta} \right\} \dots \dots \dots (4)$$

As ϵ_0 and ω are constant, we find:

$$N = E \cdot \epsilon_0 \cdot F + E (\omega - \epsilon_0) \int_{-h_2}^{h_1} \frac{\eta}{R_z + \eta} \cdot dF \dots \dots \dots (3a)$$

$$M_z = E \cdot \epsilon_0 \cdot R_z \int_{-h_2}^{h_1} \frac{\eta}{R_z + \eta} \cdot dF +$$

$$+ E\omega \int_{-h_2}^{h_1} \frac{\eta^2}{R_z + \eta} \cdot dF \dots \dots \dots (4a)$$

Suppose:

$$\int_{-h_2}^{h_1} \frac{\eta}{R_z + \eta} \cdot dF = -K \cdot F \dots \dots \dots (5)$$

then:

$$\int_{-h_2}^{h_1} \frac{\eta^2}{R_z + \eta} \cdot dF = +K \cdot F \cdot R_z \dots \dots \dots (6)$$

thus:

$$N = E \cdot \epsilon_0 \cdot F - K \cdot E \cdot F (\omega - \epsilon_0) \dots \dots \dots (3b)$$

$$M_z = K \cdot E \cdot F \cdot R_z (\omega - \epsilon_0) \dots \dots \dots (4b)$$

From (3b) and (4b) it follows that:

$$\epsilon_0 = \frac{N}{EF} + \frac{M}{EFR_z} \dots\dots\dots (7)$$

$$\omega = \frac{N}{EF} + \frac{M}{EFR_z} + \frac{M}{EFR_z K} \dots\dots (8)$$

Equations (1), (2), (7) and (8) give:

$$\sigma_\eta = \frac{1}{F} \left(N + \frac{M}{R_z} + \frac{M}{K \cdot R_z} \cdot \frac{\eta}{\eta + R} \right) \dots\dots\dots (9)$$

The neutral axis can be found by supposing $\sigma_\eta = 0$. Neglecting provisionally the term $\frac{N}{F}$ in (9), it is clear that

$$\frac{M}{R_z} + \frac{M}{KR_z} \cdot \frac{\eta}{\eta + R_z} = 0 \dots\dots (9a)$$

$$\eta_{N.A} = e = \frac{-KR_z}{K + 1} \dots\dots\dots (10)$$

From (9a) and (10) we find:

$$\sigma_{\eta_z} = \frac{M (e - \eta_z)}{F \cdot e (\eta_z + R_z)} \dots\dots\dots (11)$$

$$\frac{M}{\sigma_{\eta_z}} = W = \frac{F \cdot e (\eta_z + R_z)}{e - \eta_z} \dots\dots\dots (12)$$

η_z is the distance between the outermost layer and the centre of gravity. The only unknown factor in (12) is e , which may be deduced from (5) and (10).

This method can serve to calculate the stresses in the flanges of a curved beam in the following way (see fig. 62).

The contribution of the flanges to $-KF$ (equation 5) is obtained by:

$$\frac{\eta_{z1}}{R_z + \eta_{z1}} \cdot F_g \dots\dots\dots (13)$$

and

$$\frac{-\eta_{z2}}{-\eta_{z2} + R_z} \cdot F_k \dots\dots\dots (14)$$

For the coaming we find:

$$\begin{aligned} -KF &= t \cdot \int_{-l}^l \frac{\eta' + s}{\eta' + s + R_z} \cdot d\eta' = \\ &= t\eta' \Big|_{-l}^l - t \cdot R_z \cdot \ln (\eta' + s + R_z) \Big|_{-l}^l \\ &\quad R_z + s = R_l \end{aligned}$$

$$\begin{aligned} -KF &= t\eta' \Big|_{-l}^l - t \cdot (R_l - s) \cdot \ln (\eta' + R_l) \Big|_{-l}^l = \\ &= 2t \cdot l - t (R_l - s) \cdot \ln \frac{1 + l/R_l}{1 - l/R_l} = \end{aligned}$$

$$= 2t \cdot l - 2t (R_l - s) \left(\frac{l}{R_l} + \frac{l^3}{3R_l^3} + \frac{l^5}{5R_l^5} + \dots \right) =$$

$$\begin{aligned} &= -2t \cdot R_l \left\{ \frac{1}{3} \left(\frac{l}{R_l} \right)^3 + \frac{1}{5} \left(\frac{l}{R_l} \right)^5 + \dots \right\} + \\ &+ \frac{2 \cdot t \cdot s \cdot l}{R_l} + 2 \cdot t \cdot s \left\{ \frac{1}{3} \cdot \frac{l^3}{R_l^3} + \frac{1}{5} \cdot \frac{l^5}{R_l^5} + \dots \right\} = \end{aligned}$$

$$\begin{aligned} -KF &= \frac{2 \cdot t \cdot s \cdot l}{R_l} - 2 \cdot t (R_l - s) \\ &\left\{ \frac{1}{3} \left(\frac{l}{R_l} \right)^3 + \frac{1}{5} \left(\frac{l}{R_l} \right)^5 + \frac{1}{7} \left(\frac{l}{R_l} \right)^7 + \dots \right\} \\ &\dots\dots\dots (15) \\ &(l/R_l < 1) \end{aligned}$$

thus

$$-KF = (13) + (14) + (15)$$

and

$$e = \frac{-KR_z}{K + 1} \dots\dots\dots (10)$$

The section moduli are given by (12).

As the section of an ideal knee changes in surface, the formulae cannot be applied directly. An approximation of the problem is necessary and is given by figure 63. Here the section QZP has a straight part QZ between the centre of gravity and the curved flange, which is perpendicular to the flange. The rest of the section is formed by an arc ZP tangential to QZ and perpendicular at its end to the hull. Neglecting the orthogonal angle in the corner, it is admitted that only normal stresses σ_a act on ZP. The distribution of σ_a is assumed to be nearly that of a straight section from the curved beam having a constant section modulus equal to the section modulus of QZP.

The presence of the corner means that the real stress will be lower than σ_a , and the hypothesis is that this stress becomes $\sigma_a \cdot \cos \alpha$. Thus the cor-

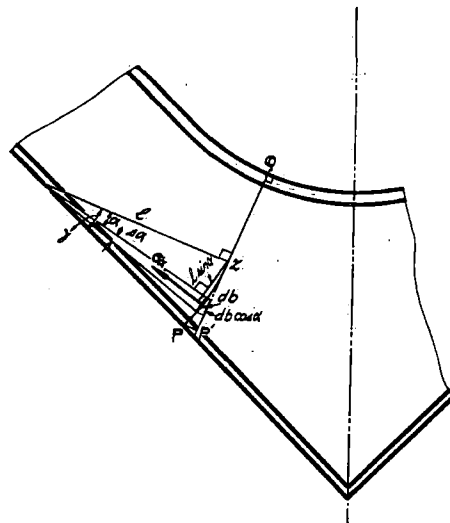


Fig. 63

TABLE III

N ^o	LENGTH OF BRACKET		THICKNESS	TYPE OF BRACKET	SYM-BOLS		
	FRAMESIDE	BEAMSIDE					
1	247	247	7,9				
2	247	247	6,35				
3	247	247	4				
6	186	186	7,9				
7	186	186	6,35				
8	186	186	4				
11	125	125	6,35				
3 ^B	247	247	3,9				
4	247	247	6,35				
10	186	186	6,35				
5	247	247	6,35				
9	186	186	6,35				
13	247	247	4				
15	186	186	4				
14	247	247	4				
16	186	186	4				
18	186	186	6,35				
12	140	210	6,35				
17	140	210	6,35				
19	186	230	6,35				
20	186	230	6,35				

rection depends on the distance between σ_a and the corner of the knee:

For db we find:

$$dM = \sigma_a \cdot \cos \alpha \cdot db \cdot l \cdot \sin \alpha.$$

But as $db \cdot \cos \alpha$ is the projection of db on QZP' and $l \cdot \sin \alpha$ is nearly the projection of the curved arc over the angle α on QZP' , we may take QZP' for QZP and calculate the latter by means of the curved beam theory. The hull flange also must be reduced by $\cos \alpha$ ($= \cos \gamma$).

Thus:

$$\sigma_p = \frac{M}{W_p'} \cdot \cos \gamma.$$

A difficulty is that Z must be taken at the centre of gravity of section QZP' . An iteration process therefore is necessary.

The result of the calculations are given in figure 13 and figure 14. The flange efficiency is taken as 90 % (see fig. 9) (see also [10] and [15]). The efficiency of the hull flange of test-piece 9 is deducted from figure 11. For type 13 this efficiency is 100 %.

APPENDIX III

SHORT ANALYSIS OF THE EXPERIMENTS AND TESTS EXECUTED IN NORWAY [12]

In 1955 a provisional report [12] was published by the Norwegian Shipbuilding Research Centre in Trondheim about the strength of bracketed connections in ships. In these tests the static compression-strength of 20 test-pieces was determined. All models were on scale 1 : 2. A certain amount of strain-gauge measurements were effected.

Table III gives a survey of the test-pieces, while in table IV the results are given.

As may be seen from table III, the Norwegian research was focussed on the determination of the influence of the size and thickness of overlapping knees on the strength of the connection. Furthermore the influence of kneeflanges, hollow knees etc. was investigated.

It is difficult to understand these influences by the use of table IV only. Because further information about the influence of bracket-thicknesses on the bracketed connection is of value and a welcome complement to the Delft tests, a further analysis of table IV is necessary.

Figure 64 gives the stress-concentration factors K_1 , K_2 and K_3 (*), the elastic limit load Q_{fl} and the maximum load Q_{max} as functions of the sizes of the knees. Figure 65 gives the same unities as function of the knee-thicknesses.

Analysing these figures 64 and 65, as well as table IV, it is clear that:

- a. The stress-concentration factor K_1 between frame and knee, is nearly independent of the kneesize. The stress-concentration factor K_2 diminishes with increasing size of the knee (see also fig. 29). With non-bevelled kneeplates, when $l = 125$ mm or $1.25 \times$ sectionheight,

$$K_2 \cong 2K_1,$$

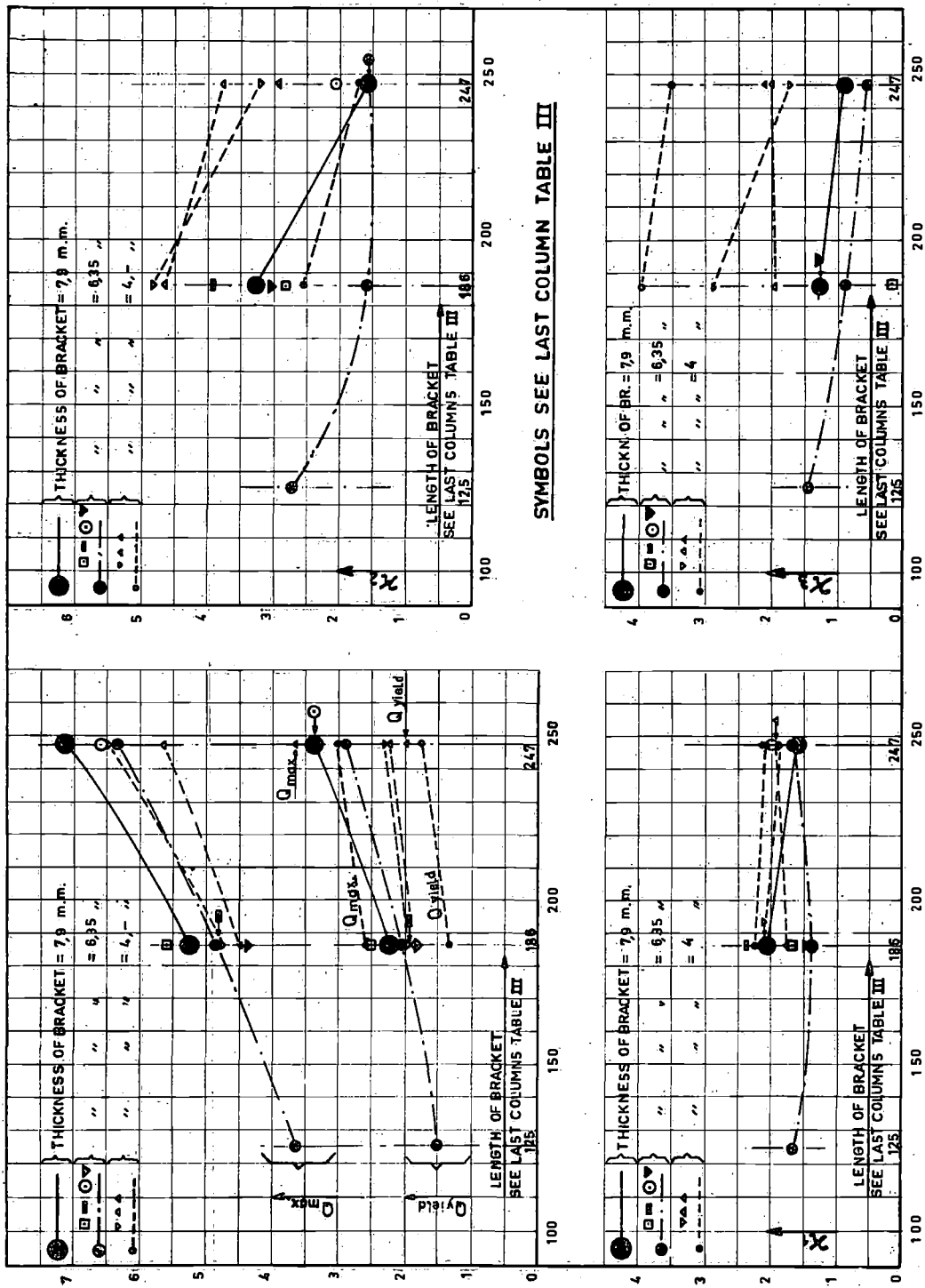
when $l = 247$ mm or $2 \times$ sectionheight,

$$K_2 \cong K_1.$$

- b. With thin bevelled knees the K_2 -values are very high (Nos. 13, 14, 15 and 16 from [12]). The K_1 -values remain normal.
- c. A butt welded kneeplate between beam and frame seems to have somewhat higher values of K_1 and K_2 in relation to an overlap-knee; this conclusion is doubtful (see end of this appendix).
- d. The plate-thickness generally has little influence on the values of K_1 and K_2 (see fig. 65), though a thickness of 0.8 times the beam-thickness, seems to give the most favorable relationship. With the Norwegian tests this knee-thickness was 6.35 mm.
- e. The stress-concentration factor K_3 diminishes slightly with increasing size of knee. Here also the most favorable relationship of kneeplate thickness to beam thickness seems to be 0.8.
- f. The limit loads Q_{fl} (***) and Q_{max} (***) rise with increasing size of knee. This rise is most accentuated between kneeplate thicknesses of 4 to 6.35 mm.
- g. A bevelled kneeplate of 4 mm is about as strong as an unbevelled kneeplate of 6.35 mm. For the bevelled kneeplate of 4 mm Q_{max} is about 1.8 times as high as for the unbevelled one of the same thickness. The Delft tests gave a difference of only 14 % between bevelled and unbevelled kneeplates of 16 mm thickness (comparable to 8 mm thickness for the Norwegian kneeplates).
- h. The test-piece 41' of the Delft series goes with the Norwegian models 1, 2, 3, 6, 7, 8 and 11. Therefore a small model scale 1 : 4 of this test-piece 41' was made in Delft. A small model 1 : 4 was also made from the test-piece 41 with bevelled kneeplate. The results of the static

*) Q_{fl} and Q_{max} are less satisfactory for judging the strength of bracketed connections. M_{fl} and M_{max} (moments) are more satisfactory in this respect.

*) For definition of K_1 , K_2 and K_3 see table IV, column 13.



SYMBOLS SEE LAST COLUMN TABLE III

Fig. 64

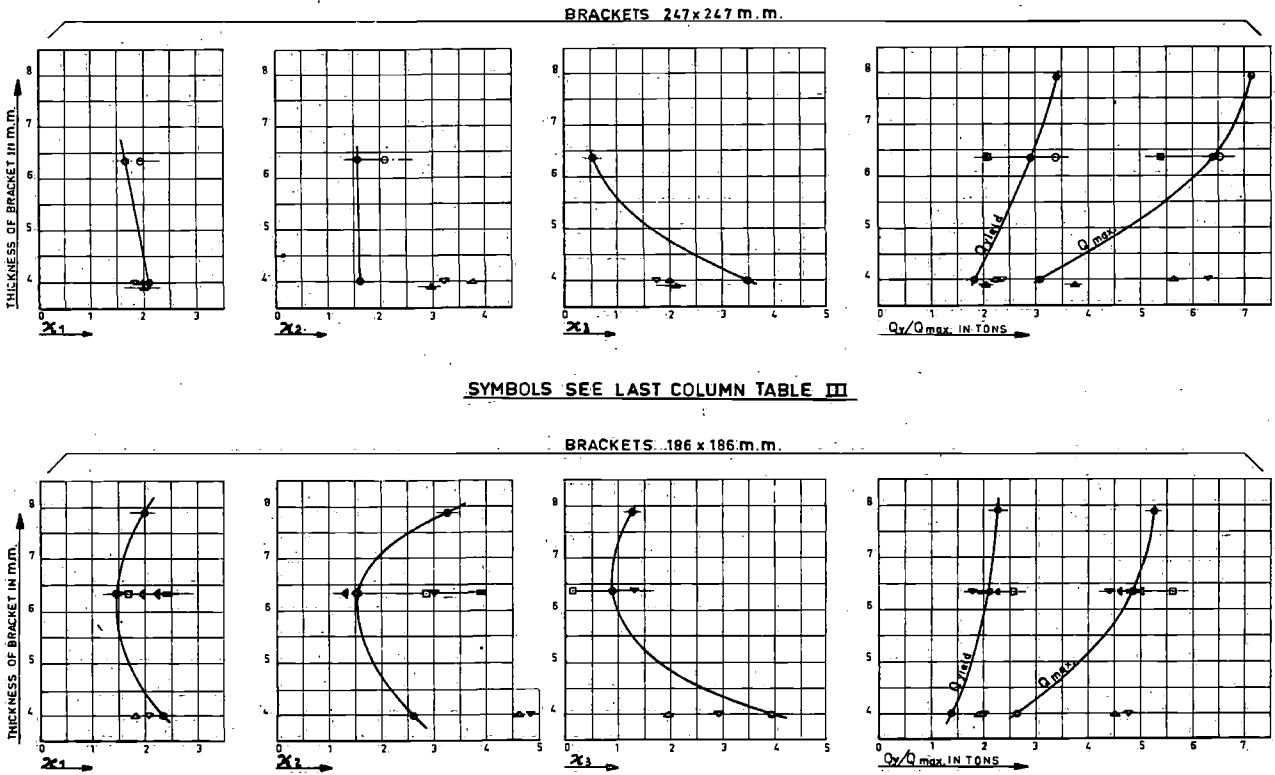


Fig. 65

compression tests with these models give us an impression about the scale effect (see table V).

TABLE V

Type	Scale	P_{max} (kg)	$P_{max} \times \left(\frac{1}{scale}\right)^2$
41'	1 : 1	22.000	22.000
	1 : 2	4.500	18.000
	1 : 4	1.000	16.000
41	1 : 1	25.000	25.000
	1 : 4	1.285	20.600
ideal knee	1 : 1	26.000	26.000
	1 : 4	1.600	25.600

It is clear that small test-pieces of types 41 and 41' are relatively less strong than big ones. This conclusion is not generally true for all small scale models as is shown by the "ideal knee". Taking the scale into account, the compression load strength of a model of the ideal knee was nearly as great as on the full-sized knee. The material of the Norwegian and the Dutch test-pieces was of the same quality.

- i. The welding of the knee or of the frame to the deckplating gives an improvement of Q_{max} of 15 % only for the small knees. For the big ones the influence is nil.
- j. In [12] a formula is given for the normal stress in the knee at half the length of the hypotenuse (see table IV column 13). This formula says:

$$\sigma_p = \frac{M \cdot k}{d^2 \cdot t}$$

For the models 1, 2, 3, 6, 7, 8 and 11 from [12] the mean value for k was 8.40. Introducing this formula in the analysis of the measurements of test-piece 41' (Dutch), one finds $k = 8.10$. The concordance is sufficient. The concordance is much less for overlapping knees with bevelled borders.

The use of stress-concentration factors as given in table IV is dangerous. These stress-concentration factors are not similar to the definitions of column 3 from table II, which indicate the local stress-concentration.

In the Norwegian tests the values of K indicate the relationship of the local stresspeak to the *calculated* stress in the sections of the beam, at the toe of the knee. The values of the stress-concentrations calculated by the factors K from

TABLE IV

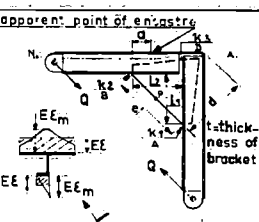
symbols	N.B.	length of bracket		thickn. of br. (t)	efficiency of:			stress concentration factor			I _m	a	Q _y	Q _{max}	K ₁	K	notes
		l ₁	l ₂		br. flange	beam fl.	plate fl.	κ ₁	κ ₂	κ ₃							
●	1	247	247	7.9						275	.91	34	7.12			820	<p>apparent point of eng. stry</p>  <p>thickness of bracket</p> <p>calculated EE_c</p> <p>measured EE_m</p> <p>efficiency = $\frac{EE}{EE_m}$; κ₁, κ₂ = $\frac{EE_m}{EE_c}$</p> <p>κ₃ = $\frac{EE \text{ measured at B}}{EE \text{ calculated at B}}$</p> <p>I_m = measured mean value of moment of inertia of framelegs</p> <p>Q_y = yield load; Q_{max} = maximum Load</p> <p>K₁ = buckling stress factor = $\frac{Q_y \cdot e^2}{t^2}$</p> <p>K = bending stress factor = $\frac{Q_p \cdot t \cdot d^2}{M}$</p> <p>Q_p = buckling stress at P</p>
	2	247	247	6.35		0.32	0.76	1.67	1.57	0.56	250	95	2.9	6.36		805	
	3	247	247	4.0		0.48	0.73	2.08	1.60	3.50	300	139	1.81	3.05	134 · 10 ⁶	793	
▲	3B	247	247	3.9		0.50	0.79	2.05	2.95	2.12	270	119	2.0	3.68	239 · 10 ⁶	765	
■	4	247	247	6.35							275	140	2.1	5.42			
○	5	247	247	6.35		0.50	0.90	1.97	2.08		280	97	3.4	6.51		690	
●	6	186	186	7.9		0.48	0.78	2.0	3.27	1.27	300	120	2.27	4.90 ⁺		9.15	
	7	186	186	6.35		0.50	0.68	1.42	1.52	0.88	290	116	2.06	4.85		8.15	
	8	186	186	4.0		0.37	0.83	2.32	2.57	3.97	295	156	1.38	2.60	136 · 10 ⁶	787	
□	9	186	186	6.35		0.54	0.84	1.65	2.85	0.16	275	88	2.54	5.60		6.78	
▽	10	186	186	6.35		0.58	0.75	1.49	3.00	1.30	275	116	1.80	4.38		9.00	
●	11	125	125	6.35		0.56	0.66	1.64	2.72	1.48	280	159	1.51	3.60		9.60	
▲	12	140	210	6.35		0.54	0.84	2.50	3.20	1.18	260	137 ^x	2.30	4.25		6.76	
▽	13	247	247	4.0	0.52	0.50	0.86	3.75 [*]	1.96	2.00	250	95	2.22	5.60		6.54	
▽	14	247	247	4.0	0.50	0.49	0.76	1.90	3.25	1.74	265	95	2.30	6.32		2.45	
▲	15	186	186	4.0	0.34	0.51	0.75	1.77	4.60	1.94	280	112	1.89	4.48		2.31	
▽	16	186	186	4.0	0.55	0.50	0.77	2.07	4.80	2.90	275	119	1.98	4.76		2.63	
▽	17	140	210	6.35	0.50	0.50	0.75	1.60	2.77	1.13	250	115 ^x	3.02	4.83		1.77	
■	18	186	186	6.35		0.50	0.76	2.40	3.90		290	118	1.96	4.82		6.90	
▲	19	186	230	6.35		1.00	0.74	2.25	1.29		225	128 ^x	1.98	4.56		5.90	
▽	20	186	230	6.35	1.00	1.00	0.75	1.53 ⁺	1.91		225	122 ^x	2.26	5.00		1.48	

table IV can be transformed to local stress-concentrations by multiplying the Norwegian K-values by 0.65 for L-sections and by 0.88 for T-sections.

The strain-gauges used in Norway and in Delft were of the same size. But as the scale of the models in Norway was scale 1 : 2 and in Delft they were full-scale, the measurement of stress-concentrations in Norway was less exact. Moreover the location of the strain-gauges is of importance (see tables II and IV and fig. 42); this is shown clearly in figure 66. The stress is much lower in the immediate vicinity of the weld than in the weld.

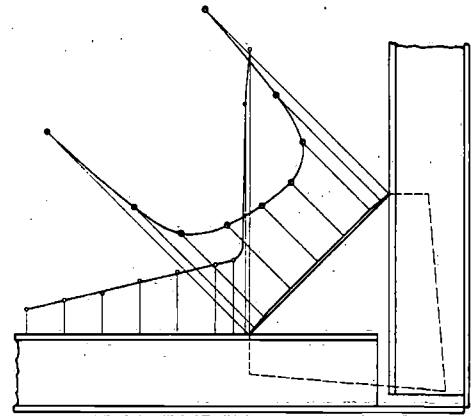


Fig. 66. Knee nr. 15 [12]